Original Article

Diagnostics and immunological function of CENPN in human tumors: from pan-cancer analysis to validation in breast cancer

Yubo Jing[#], Yiyang Wang[#], Yongxiang Li, Xinzhu Huang, Junyi Wang, Dlraba Yelihamu, Chenming Guo

Department of Breast Surgery, Center of Digestive and Vascular, The First Affiliated Hospital of Xinjiang Medical University, Urumqi, China

Contributions: (I) Conception and design: Y Jing, C Guo; (II) Administrative support: C Guo; (III) Provision of study materials or patients: Y Jing, Y Wang; (IV) Collection and assembly of data: X Huang, D Yelihamu, J Wang; (V) Data analysis and interpretation: X Huang, Y Wang, Y Li; (VI) Manuscript writing: All authors; (VII) Final approval of manuscript: All authors.

[#]These authors contributed equally to this work.

Correspondence to: Chenming Guo, MD. Department of Breast Surgery, Center of Digestive and Vascular, The First Affiliated Hospital of Xinjiang Medical University, 137 Liyushan Rd., Urumqi 830054, China. Email: gcm_xjmu@yeah.net.

Background: Centromere protein N (*CENPN*), a member of the centromere protein family, contributes to ribonucleic assembly, mitosis progression, and chromosome separation. *CENPN* manifests a close link with the occurrence and progression of several malignant cancers, but there is no pan-cancer study on *CENPN*, and we aim to ascertain the connection between *CENPN* and human cancer prognosis and immunotherapy.

Methods: The *CENPN* function in multiple malignant tumors was comprehensively investigated with data from The Cancer Genome Atlas (TCGA) and integrated Gene Expression Omnibus (GEO) database. We examined the transcriptional level, prognostic effect, diagnostic value, genetic and epigenetic alteration, methylation level, and immunological importance of *CENPN*. Furthermore, this work provided further confirmation of the phenotypic regulating function of *CENPN* in breast cancer (BC) cells.

Results: *CENPN* exhibited significant upregulation in diverse cancer tissues and had different expression patterns across immunological and molecular subgroups in several cancer types. Elevated expression of *CENPN* may correlate with a worse prognosis. *CENPN* effectively differentiates most cancers from healthy tissues. Hypomethylate was shown to be *CENPN* promoter in most cancers. *CENPN* was shown to be connected with levels of different immune cell infiltration. Kyoto Encyclopedia of Genes and Genomes (KEGG) and the Gene Set Enrichment Analysis (GSEA) analysis suggested that *CENPN* may mediate neutrophil extranuclear trap formation, cell cycle, and p53 signaling pathways in cancer. *In vitro* studies showed that the overexpression of *CENPN* promotes the proliferation, invasion, and migration of BC cells, while concurrently inhibiting their apoptosis.

Conclusions: *CENPN* may operate as a novel predictive indicator and molecular target for targeted therapy in pan-cancer. Significantly, *CENPN* contributed to controlling the BC growth and advancement.

Keywords: Pan-cancer; centromere protein N (*CENPN*); cell cycle; tumor immunity; methylation

Submitted Sep 25, 2024. Accepted for publication Jan 03, 2025. Published online Feb 26, 2025.
doi: 10.21037/tcr-24-1291
View this article at: https://dx.doi.org/10.21037/tcr-24-1291

Introduction

Cancer is becoming a global problem affecting human health, a leading cause of death in every country, and a significant obstacle to improving life expectancy (1). Cancer treatment has long been a crucial and significant clinical issue, and anti-tumor approaches encompassing surgery, radio-, chemo- and immunotherapy have been extensively used in clinical settings, yet the treatment effect of most tumors is still suboptimal (2).

Centromere-associated proteins (*CENPs*) are a group of proteins involved in assembling the centromere,

© AME Publishing Company.

containing 18 protein isoforms, which dynamically bind and separate from centromeric chromatin during cellular mitosis and precisely regulate cellular mitosis (3). Centromere protein N (*CENPN*) belongs to the centromere family and has an essential involvement in nuclear assembly, mitotic progression, and chromosome segregation (4,5). It has been emphasized that *CENPN* may involve in developing and progressing multiple cancers. It has been confirmed that *CENPN* contributes to the breast cancer (BC) tumor progression, thereby affecting the prognosis of BC patients (6). In lung adenocarcinoma (LUAD), *CENPN* is thought to promote tumor progression by positively modulating the phosphoinositide 3-kinase/protein kinase B (*PI3K/AKT*) pathway (7). *CENPN* can also increase the nasopharyngeal carcinoma cells' growth and proliferation and, at the same time, affect paclitaxel (PTX) resistance by inhibiting the cyclic-AMP response binding protein-vesicle-associated membrane protein 8 (*CREB-VAMP8*) signaling axis (8). *CENPN* has also been found to be involved in developing cancers such as liver cancer (9), esophageal cancer (ESCA) (10), and gastric adenocarcinoma (11). Although a growing body of research has demonstrated the *CENPN* function in cancer, there are no pan-cancer studies on *CENPN*. We aimed to estimate the link between *CENPN* and prognosis and immunotherapy in human cancer.

To illustrate the biological importance of *CENPN* in cancer, we conducted an examination of *CENPN* using several databases. We examined the *CENPN* expression in 33 different cancer types and evaluated the prognostic significance of *CENPN* using a publicly available database. Additionally, we examined its correlation with immune cell infiltration and conducted an examination to identify functional enrichments. Simultaneously, we were investigating the significant contribution of *CENPN* in BC using *in vitro* research. Our findings enhance our comprehension of the *CENPN* function in tumors and highlight that *CENPN* affects cancer patient outcomes and may operate as a possible target for future treatment. We present this article in accordance with the MDAR and TRIPOD reporting checklists (available at https://tcr.amegroups.com/article/view/10.21037/tcr-24-1291/rc).

Highlight box

Key findings

- Centromere protein N (CENPN) may serve as a new potential prognostic marker for malignancies and a potential molecular target for targeted therapies.

What is known and what is new?

- CENPN may be involved in the occurrence and progression of a variety of cancers, including liver cancer, esophageal cancer, and gastric adenocarcinoma.
- The high expression of CENPN promoted the proliferation, invasion and migration of breast cancer cells, and inhibited the apoptosis of breast cancer cells.

What is the implication, and what should change now?

- CENPN levels may have important prognostic value for invasive cancers and may become a new target for cancer immunotherapy.

Methods

CENPN expression

UCSC XENA (https://xenabrowser.net/datapages/) was implemented to acquire the ribonucleic acid (RNA) sequencing and associated clinical data from the pan-cancer cohort (n=15,776). This database contains data from The Cancer Genome Atlas (TCGA) and normal tissue specimens from the Genotype-Tissue Expression (GTEx) database (12). The study was conducted in accordance with the Declaration of Helsinki (as revised in 2013).

CENPN diagnostic and prognostic values examination

The link between the *CENPN* messenger RNA (mRNA) expression level and the patient's prognosis with each tumor was examined by the Cox regression model. The prognostic indicators considered for patients were overall survival (OS), disease-specific survival (DSS), and progression-free survival (PFS). The Cox regression analysis and charting of Kaplan-Meier (KM) survival curves (13) were implemented with the "survival" and "survminer" packages. The forest and Venn plots for the finding's visualization were generated by the "ggplot2" package.

The KM Plotter (https://kmplot.com/analysis/) and PrognoScan databases (http://dna00.bio.kyutech.ac.jp/PrognoScan/index.html) were implemented for additional investigation of survival prognosis. Eleven datasets involving four tumors were analyzed using the PrognoScan database to validate further the link between *CENPN* expression and the survival and prognosis of patients with bladder urothelial carcinoma (BLCA), LUAD, breast invasive carcinoma (BRCA), and glioblastoma multiforme (GBM).

The "pROC" package was used for doing receiver operating characteristic (ROC) analysis, whereas the

© AME Publishing Company.

"ggplot2" package was applied for results visualization. An area under the ROC curve (AUC) values between 0.7 and 0.9 suggests that *CENPN* has moderate diagnostic potential, whereas an AUC value >0.9 suggests high diagnostic potential.

Development and calibration of nomograms

Initially, we evaluated the risk factors that influenced the patient's prognosis by using univariate and multivariate Cox regressions. Consequently, only variables with P values below 0.1 were used for the following multivariate Cox analyses. The *CENPN* expression was allocated into high- and low-expression groups, using the average as the threshold. It was subsequently added as an independent factor. The nomogram was constructed by incorporating the chosen criteria from the multivariate Cox regression analysis. The consistency index (C-index) was applied to ascertain the nomogram's prediction accuracy with 1,000 repeats. Calibration curves were created to compare the projected and actual operating systems.

Functional and pathway of protein interactions and enrichment analysis

The STRING (search tool for the retrieval of interacting genes/proteins) database (https://cn.string-db.org/) was implemented to create and visualize the interaction network of *CENPN*-linked functional proteins and to explore the interaction between *CENPN* and linked proteins. The primary biological involvements of *CENPN* and its linked proteins, as well as the predicted pathways and related functions, were examined by Gene Ontology (GO) and the Kyoto Encyclopedia of Genes and Genomes (KEGG). Then, the enrichment of the differentially expressed gene in the pathway was verified with the Gene Set Enrichment Analysis (GSEA) (14).

CENPN methylation analysis

Herein, we applied The University of Alabama at Birmingham Cancer Data Analysis Portal (UALCAN) database (http://ualcan.path.uab.edu/index.html) (15) to perform a comparative examination of the *CENPN* promoter methylation levels in various types of malignancies, using both normal and TCGA samples.

CENPN genetic alteration analysis

In this study, we used the cBioPortal database (http://www.cbioportal.org/) (16) and specifically the "onponcoprint" module (https://www.cbioportal.org) to identify the extent of genetic alterations in the *CENPN* gene within the "TCGA pan-cancer atlas studies" dataset (17). The "cancer types summary" module was applied to evaluate alterations in *CENPN*, the number of gene mutations, the sorts of mutations, and the recurrence of copy number variants (CNVs) in each cancer. The "mutation" module was used to assess the *CENPN* mutation sites and was confirmed in its protein three-dimensional structure. In pan-cancer, each CNV and single nucleotide variation (SNV) type's *CENPN* percentage was acquired from the catalog of somatic mutations in cancer (COSMIC) (https://cancer.sanger.ac.uk/cosmic) (18).

CENPN immune mechanism analysis

The connection between *CENPN* and tumor mutational burden (TMB), microsatellite instability (MSI), and neocancer antigen (NEO) in several cancers was examined using the Sangerbox3.0 (http://vip.sangerbox.com/) online database. "GSVA" and "org. The Hs.eg .db" tools were used for tumor stromal, immune invasion, and tumor purity scores. The genes list for immune activators, immunosuppression, chemokines, chemokine receptors, and major histocompatibility complex (MHC) molecules were acquired from the GSEA database (https://www.gsea-msigdb.org/gsea/msigdb/index.jsp). In this work, we implemented the Tumor Immune Dysfunction and Exclusion (TIDE) algorithm to determine the connection between *CENPN* expression and immunosuppression. Moreover, the Spearman correlation coefficient was applied to detect the correlation between *CENPN* expression levels and immune-related gene expression.

In the pan-cancer, the 24 immune cell infiltration levels were assessed with the single-sample GSEA (ssGSEA) algorithm (19). The link between *CENPN* expression and immune cell infiltration levels was examined with Estimating the Proportion of Immune and Cancer cells (EPIC), Tumor Immune Estimation Resource (TIMER), Cell-Type Identification by Estimating Relative Subsets of RNA Transcripts (CIBERSORT), and MCPCOUNTER (http://timer.cistrome.org/) of the "immune" module in the

© AME Publishing Company.

TIMER2.0 database.

Cell culture and transfection

The MDA-MB-231 cell line (CL-0150B, Procell Life Science & Technology Co., Ltd., China) was cultivated at 37 ℃ with a 5% concentration of CO_2 in DMEM (PM150210, Procell Life Science & Technology Co., Ltd.) enriched with 10% fetal bovine serum (FBS) (10091148, Gibco, Suzhou, China), 100 μg/mL of streptomycin and penicillin (SV30010, Hyclone, Logan, UT, USA). Lipofectamine 3000 (L3000015, Invitrogen, Carlsbad, CA, USA) was applied to transfect the MDA-MB-231 cells with a plasmid aligning with the manufacturer's recommendation. Transfected cells were gathered 48 h later for examination using quantitative real-time polymerase chain reaction (qRT-PCR) and Western blotting.

Western blot

The MDA-MB-231 cells were broken down using an ice-cold RIPA Buffer (PR20001, Proteintech, Wuhan, China) that was mixed with a protease inhibitor cocktail (4693116001, Sigma, St. Louis, MO, USA). The mixture was then placed on ice for 30 min. The specimens were placed in a 10-minute boiling process in water containing protein loading buffer (P1040, Solarbio, Beijing, China). Afterward, they were loaded into a 10% SDS-PAGE gel and deposited onto polyvinylidene fluoride (PVDF) membranes with a thickness of 0.45 mm (ISEQ00010, Millipore, Burlington, MA, USA). The PVDF membranes were obstructed for 1 h at ambient temperature and thereafter incubated with primary antibodies overnight at 4 ℃ specific to *CENPN* (anti-*CENPN*, 1:×000, antibody produced in rabbit/mouse, 16751-1-AP, Proteintech) and ACTIN (1:5,000, antibody produced in rabbit, 20536-1-AP, Proteintech). Subsequently, this was incubated with a horseradish peroxidase-conjugated secondary antibody at a dilution of 1:10,000 (anti-rabbit, SA00001-2, Proteintech or anti-mouse, AS003, ABclonal, Wuhan, China) for 45 min at ambient temperature. Next, the membranes were observed with the enhanced chemiluminescence (ECL) reagent (P0018FM, Beyotime, Shanghai, China) by chemiluminescence.

Cell proliferation assay

The cell proliferation experiment was conducted with the cell counting kit-8 (CCK-8, 40203 ES 76, Yeasen, Shanghai, China). In summary, two distinct cell types were distributed evenly in 24 well plates at the proper volume for each well. Cells from both the control and experimental groups were treated as appropriate, while the medium without cells was utilized as a blank control. Following incubation at 37 ℃ and a CO_2 concentration of 5% for 0, 24, 48, and 72 h, a 10 μL solution of CCK-8 was introduced and then incubated for an extra time for 3 h at 37 ℃. Afterward, a microplate reader (ELX800, Biotek, USA) was implemented to ascertain the cell's optical density at 450 nm. The Annexin V-APC/7-ADD cell apoptosis detection kit (40304 ES 60, Yeasen) was applied to identify cell apoptosis. Two distinct cell types were placed in 6-well plates and subjected to appropriate treatments. The treated and control cells were exposed to 5 μL of Annexin V-APC for 15 min and 10 μL of PI reagent for 15 min in a light-restricted environment. The level of apoptosis was then determined by flow cytometry (BD FACSCanto, GE Healthcare, Piscataway, NJ, USA).

Cell Invasion and migration assay

Transwell chambers (3422, Corning, USA) were implemented to conduct *in vitro* cell invasion and migration tests. An 8-μm filter was used to introduce transfected and controlled MDA-MB-231 cells into transwell chambers either with or without matrigel. Afterward, we introduced the medium comprising 10% FBS to a Transwell chamber that was filled with 600 μL (10091148, Gibco). This chamber was then put in the bottom chamber as a chemoattractant and incubated for 24 h at 37 ℃ in an environment with 5% CO_2. Then, a cotton swab was applied to remove the remaining cells located on the insert membrane's top surface. The total cell number entered into the bottom chamber was subsequently immobilized using a 4% paraformaldehyde solution (P0099, Beyotime) for 30 min. Afterward, the immobilized cells were treated with a 0.1% crystal violet fixation solution (C0121, Beyotime). The invasive and migratory cells were examined and quantified at a magnification of 200× using an inverted microscope (MF52-N, Mshot, Guangzhou, China). Each specimen was repeated 3 times during the cell experiment.

Statistical analysis

The statistical analysis was implemented with R software version 4.0.3 (https://www.R-project.org/). The data visualization was implemented using the "ggplot2" package.

© AME Publishing Company.

The Mann-Whitney *U* and Wilcoxon signed-rank tests were applied to analyze changes in the *CENPN* in unpaired and paired samples, respectively. The Spearman correlation coefficient was used to examine the relationship between *CENPN* expression and N6-methyladenosine (m6A) methylation regulators, TMB, MSI, immunological score, and immune-linked genes. A P value <0.05 was considered to be significant.

Results

CENPN expression in pan-cancer and its subtypes

We ascertained the *CENPN* mRNA expression level in varying human malignancies through the TCGA database. The outcomes found that *CENPN* mRNA expression was greater in tumor tissues, including BLCA, BRCA, cervical squamous cell carcinoma and endocervical adenocarcinoma (CESC), cholangiocarcinoma (CHOL), colon adenocarcinoma (COAD), ESCA, GBM, head and neck squamous cell carcinoma (HNSC), liver hepatocellular carcinoma (LIHC), LUAD, lung squamous cell carcinoma (LUSC), prostate adenocarcinoma (PRAD), rectum adenocarcinoma (READ), stomach adenocarcinoma (STAD), and uterine corpus endometrial carcinoma (UCEC) tissues (P<0.05) and lower in thyroid carcinoma (THCA) tumor tissues than the corresponding normal tissues (P<0.05; *Figure 1A*). Because of the few corresponding normal tissue data for some tumors in the TCGA database, to be more convincing, we included the normal samples in the GTEx database. The outcomes emerged that *CENPN* mRNA expression did not differ significantly among the four malignant tumor tissues: mesothelioma (MESO), pheochromocytoma and paraganglioma (PCPG), sarcoma (SARC), and uveal melanoma (UVM). Except for *CENPN* mRNA low expression in acute myeloid leukemia (LAML) contrasted with normal tissues (P<0.05), the remaining 28 malignant tumor tissues found a significant elevation in the *CENPN* mRNA expression (P<0.05; *Figure 1B*). Furthermore, after confirming paired samples of 23 malignancies, we concluded that BLCA, BRCA, CHOL, HNSC, kidney renal clear cell carcinoma (KIRC), and *CENPN* mRNA in LIHC, LUAD, LUSC, PRAD, READ, STAD and UCEC in THCA (P<0.05; *Figure 1C*).

Furthermore, we emerged a direct correlation between the *CENPN* expression at different stages of tumor development and an escalation in the expression level of advanced malignancies in increased tumors, such as adrenocortical carcinoma (ACC) (*Figure 2A*), BRCA (*Figure 2B*), kidney renal papillary cell carcinoma (KIRP) (*Figure 2C*), and LUAD (*Figure 2D*). This shows that *CENPN* could be used as an essential indicator of advanced prognosis in these malignancies.

We ascertained the differential CENPN expression in multiple pan-cancer immunology and molecular subtypes using the TISIDB database. *CENPN* expression in 14 cancer subtypes with different molecular subtypes. For cancer types with elevated *CENPN* expression, CpG Island Methylator Phenotype (CIMP)-high subtype of ACC (*Figure 2E*), Basal subtype of BRCA (*Figure 2F*), HM-SNV subtype of COAD (*Figure 2G*), ESCC subtype of ESCA (*Figure 2H*), C2c-CIMP subtype of KIRP (*Figure 2I*), G-CIMP-low subtype of brain lower grade glioma (LGG) (*Figure 2J*), iCluster:3 subtype of LIHC (*Figure 2K*), classical subtype of LUSC (*Figure 2L*), immunoreactive subtype of ovarian serous cystadenocarcinoma (OV) (*Figure 2M*), cortical admixturre subtype of PCPG (*Figure 2N*), 5-speckle-type pox virus and zinc finger protein (SPOP) subtype of PRAD (*Figure 2O*), hotspot subtype of skin cutaneous melanoma (SKCM) (*Figure 2P*), Epstein-Barr virus (EBV) subtype of STAD (*Figure 2Q*) and polymerase epsilon (POLE) subtype of UCEC (*Figure 2R*) showed the most significant expression of *CENPN*.

In addition, our analysis classified tumors into 6 immune subtypes. The *CENPN* expression was significantly linked to multiple immune subtypes of 19 malignant tumors, including ACC, BLCA, BRCA, COAD, ESCA, KIRC, KIRP, LGG, LIHC, LUAD, LUSC, OV, pancreatic adenocarcinoma (PAAD), PRAD, READ, SARC, STAD, UCEC and UVM (*Figure 2S*). In a variety of cancers, *CENPN* is the least expressed in the C3 (inflammatory) immune subtype. Briefly, the immune and molecular subtypes exhibit different *CENPN* expressions.

CENPN predictive and diagnostic significance in pan-cancer

To better understand whether *CENPN* expression impacts the cancer patient's prognosis, we executed a survival analysis of *CENPN* expression in cancer patients using a prognostic scan database. Four cancers, including BLCA, LUAD, BRCA, and GBM, were validated by 11 datasets (GSE13507, GSE13213, GSE31210, GSE1456, GSE4922, GSE2990, GSE7390, GSE12276, GSE2034, GSE4271, and GSE4412). Moreover, it was found that for patients with these four cancers, high *CENPN* expression exhibited a worse connection with prognosis (Cox P<0.05; *Figure 3*).

© AME Publishing Company.

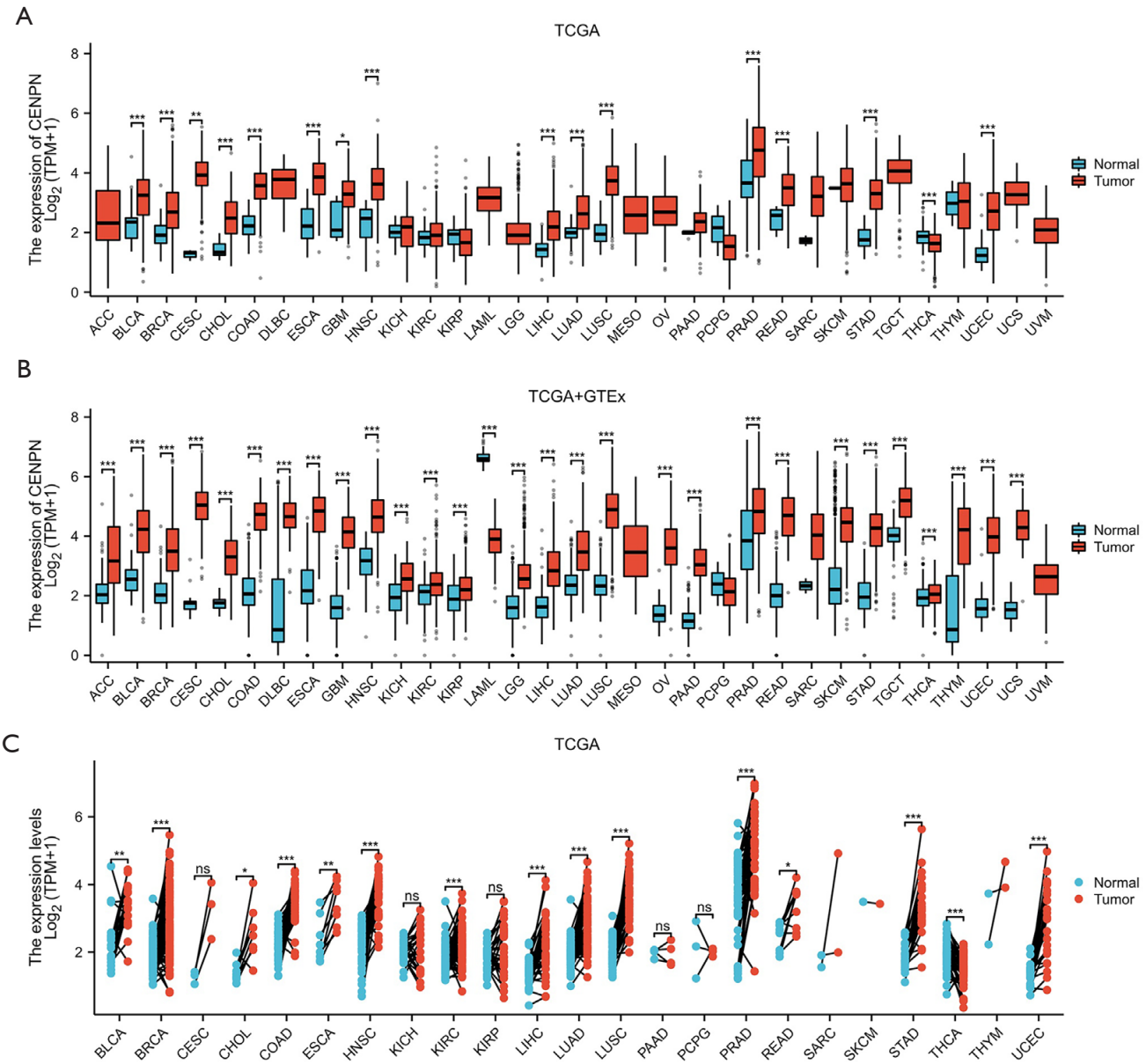

Figure 1 Variations in CENPN expression among the 33 cancers. (A) CENPN mRNA expression difference between TCGA tumor and normal tissues. (B) Tumor and normal tissues with data from TCGA and GTEx. (C) TCGA tumor and paired normal tissues. ns, not significant; *, P<0.05; **, P<0.01; ***, P<0.001. GTEx, the genotype-tissue expression; mRNA, messenger RNA; TCGA, The Cancer Genome Atlas; TPM, transcripts per million.

We used the TCGA database to determine the predictive significance of *CENPN* in pan-cancer, including three prognostic indicators (OS, PFS, and DSS). For OS (Figure S1A), we found that *CENPN* high expression was responsible for ACC [hazard ratio (HR) =4.91, 95% confidence interval (CI): 2.07–11.68], BRCA (HR =1.47, 95% CI: 1.07–2.02), LGG (HR =2.30, 95% CI: 1.58–3.36), LUAD (HR =1.54, 95% CI: 1.15–2.06), and MESO (HR =3.13, 95% CI: 1.88–5.21), PAAD (HR =1.67, 95% CI: 1.10–2.53), and SARC (HR =1.58, 95% CI: 1.06–2.35) were unfavorable factors for shorter OS (*Figure 4A*). For PFS (Figure S1B), high *CENPN* expression was linked to ACC (HR =3.15, 95% CI:

© AME Publishing Company.

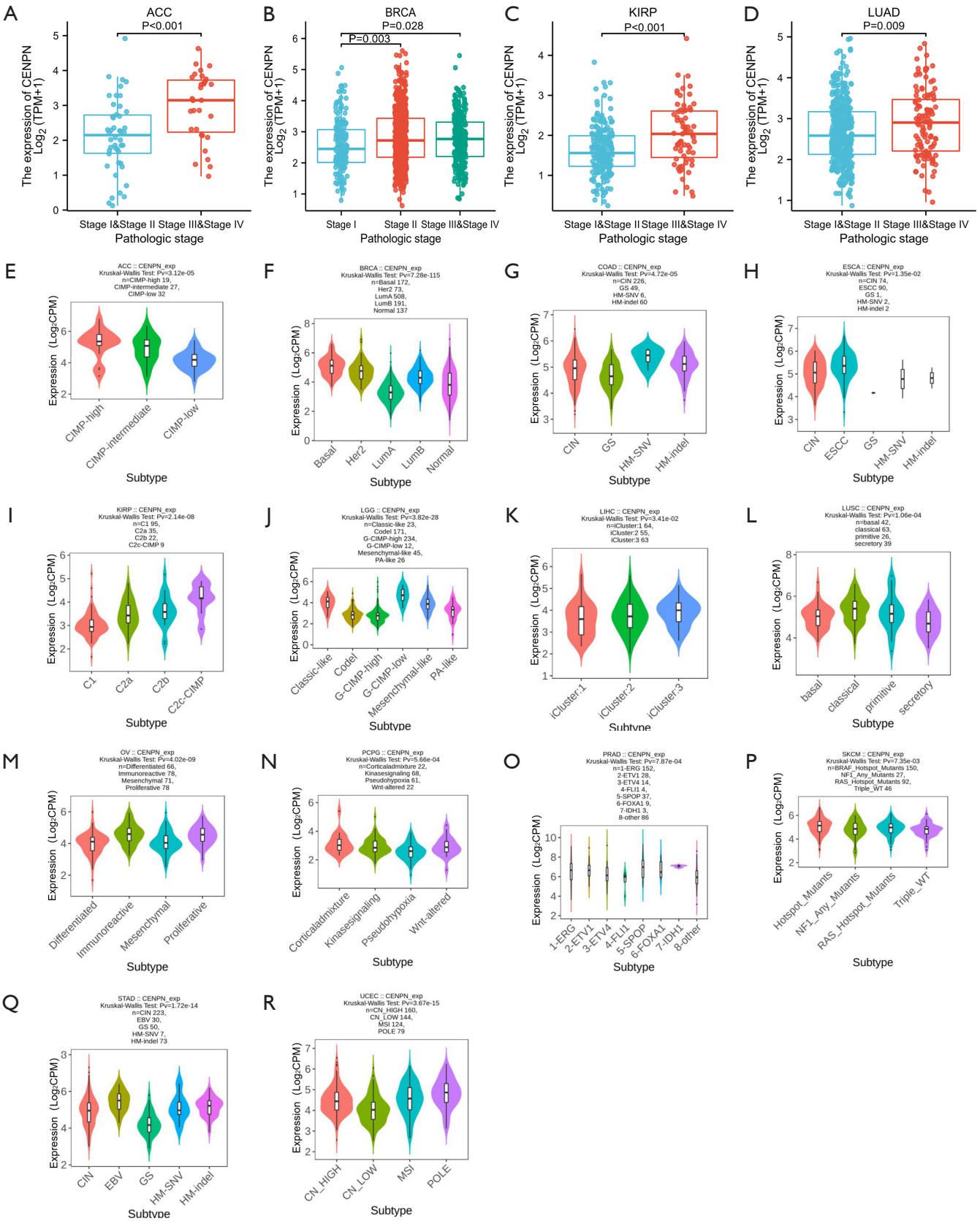

© AME Publishing Company.

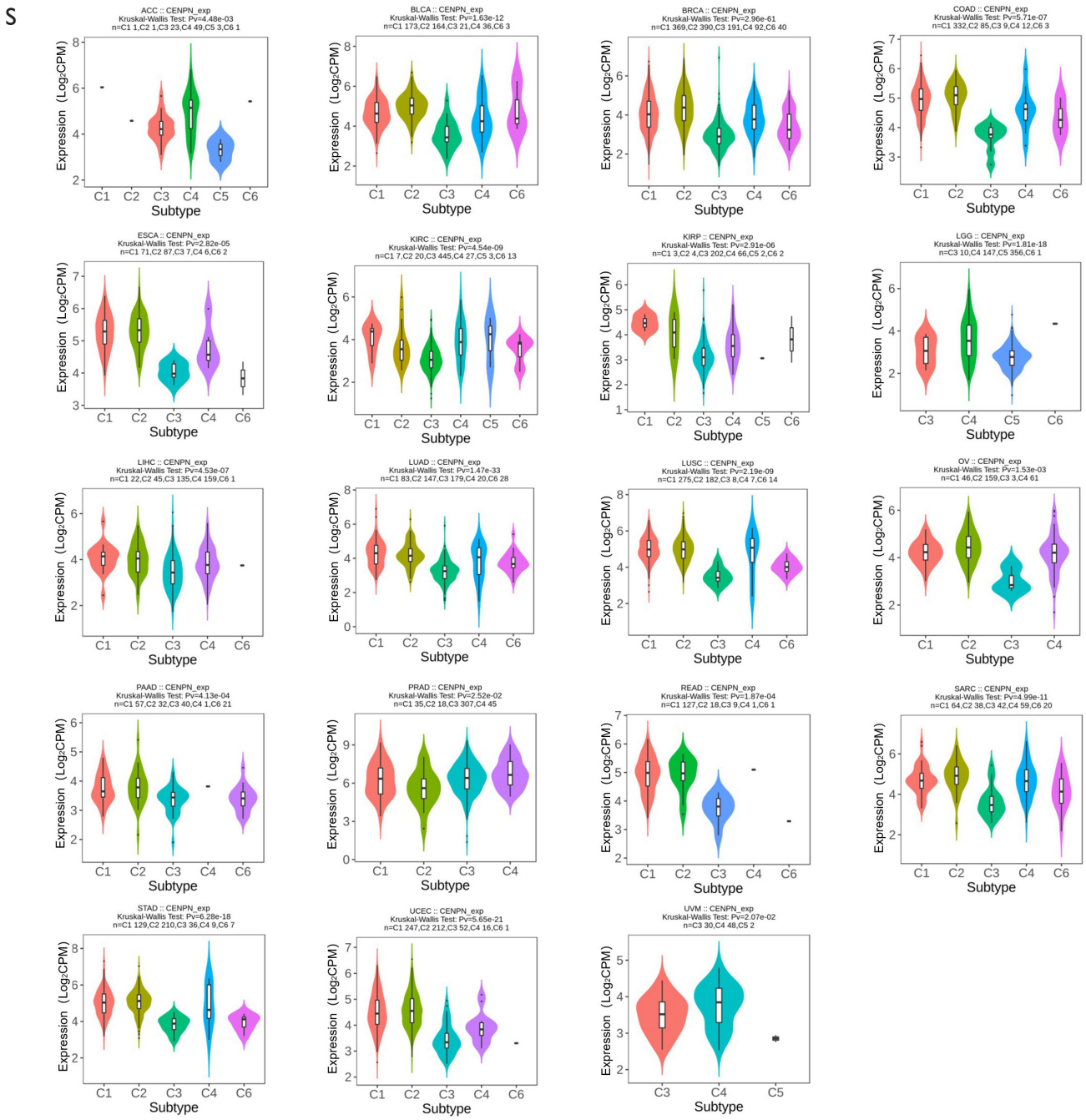

Figure 2 The connection between CENPN expression and a variety of tumor stages, molecular, and immune subtypes. Connection between CENPN expression and various tumor stages, encompassing (A) ACC, (B) BRCA, (C) KIRP, and (D) LUAD. Connections between molecular subtypes and CENPN expression between TCGA tumors, encompassing (E) ACC; (F) BRCA; (G) COAD; (H) ESCA; (I) KIRP; (J) LGG; (K) LIHC; (L) LUSC; (M) OV; (N) PCPG; (O) PRAD; (P) SKCM; (Q) STAD; (R) UCEC. (S) Relationships between immune subtypes and CENPN expression between TCGA tumors, encompassing ACC, BLCA, BRCA, COAD, ESCA, KIRC, KIRP, LGG, LIHC, LUAD, LUSC, OV, PAAD, PRAD, READ, SARC, STAD, UCEC, and UVM. C1, wound healing; C2, IFN-γ dominant; C3, inflammatory; C4, lymphocyte depletion; C5, immunologically quiet; C6, TGF-β dominant; CPM, counts per million; CIN, chromosomal instability; CIMP, CpG Island Methylator Phenotype; CN, copy number; ESCC, esophageal squamous cell carcinoma; EBV, Epstein-Barr virus; GS, genomically stable; HM-SNV, hypermutated-single nucleotide variation; MSI, microsatellite instability; TCGA, The Cancer Genome Atlas; TPM, transcripts per million.

© AME Publishing Company.

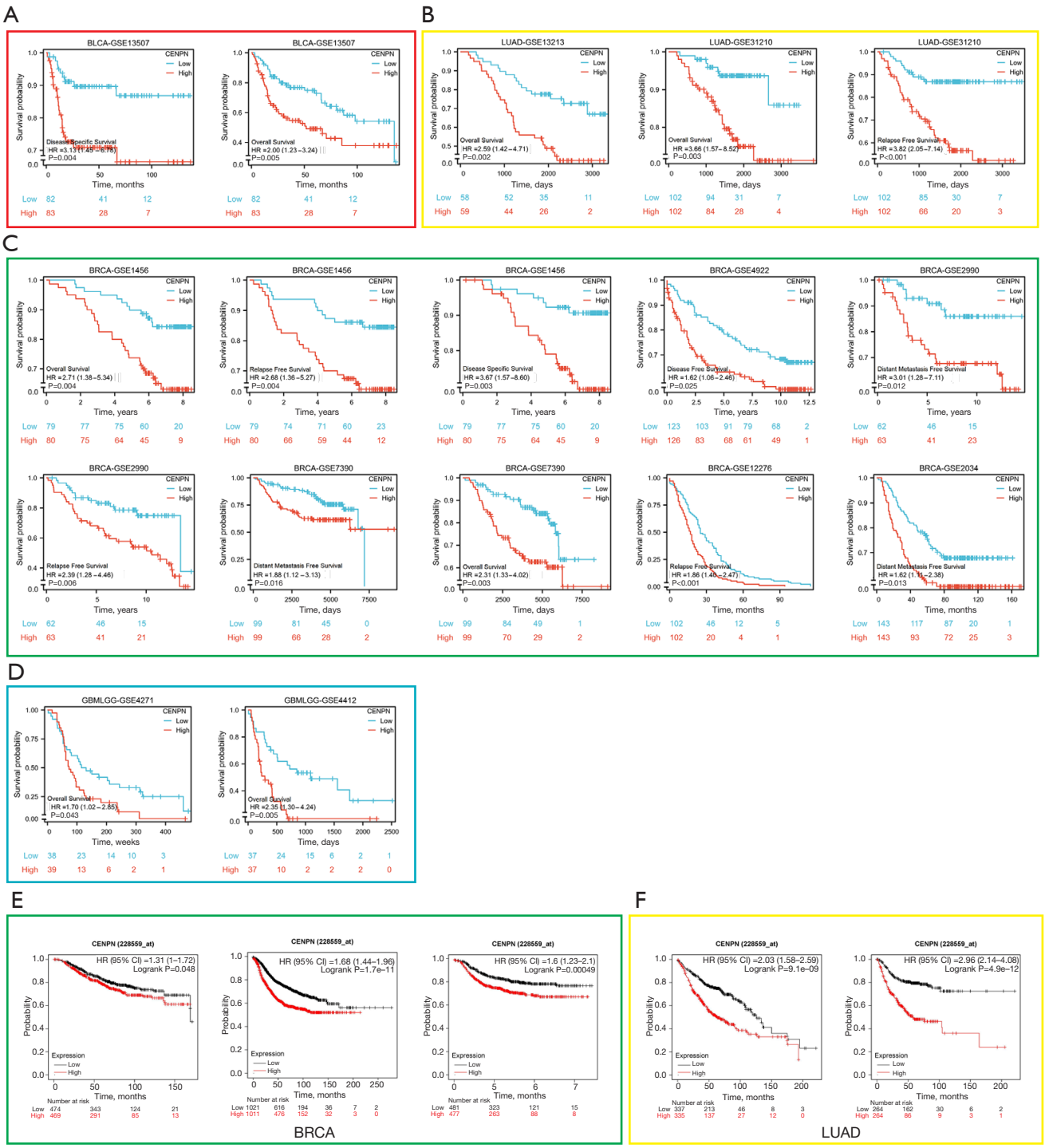

Figure 3 CENPN survival analysis among a variety of cancer types in GEO and TCGA datasets. (A) Kaplan-Meier plots of CENPN in 11 datasets encompassing GSE13507, BLCA, OS, and DSS; (B) GSE13213, GSE31210, LUAD, OS and RFS; (C) GSE1456, GSE4922, GSE2990, GSE7390, GSE12276, GSE2034, BRCA OS, RFS, DSS, DFS, and DMFS; (D) GSE4271, GSE4412, GBMLGG, OS; (E) BRCA, OS, RFS, and DMFS; (F) LUAD, OS and first progression. Values in parentheses represent the 95% confidence interval. CI, confidence interval; DFS, disease-free survival; DMFS, distant metastasis free survival; DSS, disease-specific survival; GEO, Gene Expression Omnibus; GBMLGG, glioma; HR, hazard ratio; OS, overall survival; RFS, relapse-free survival; TCGA, The Cancer Genome Atlas.

© AME Publishing Company.

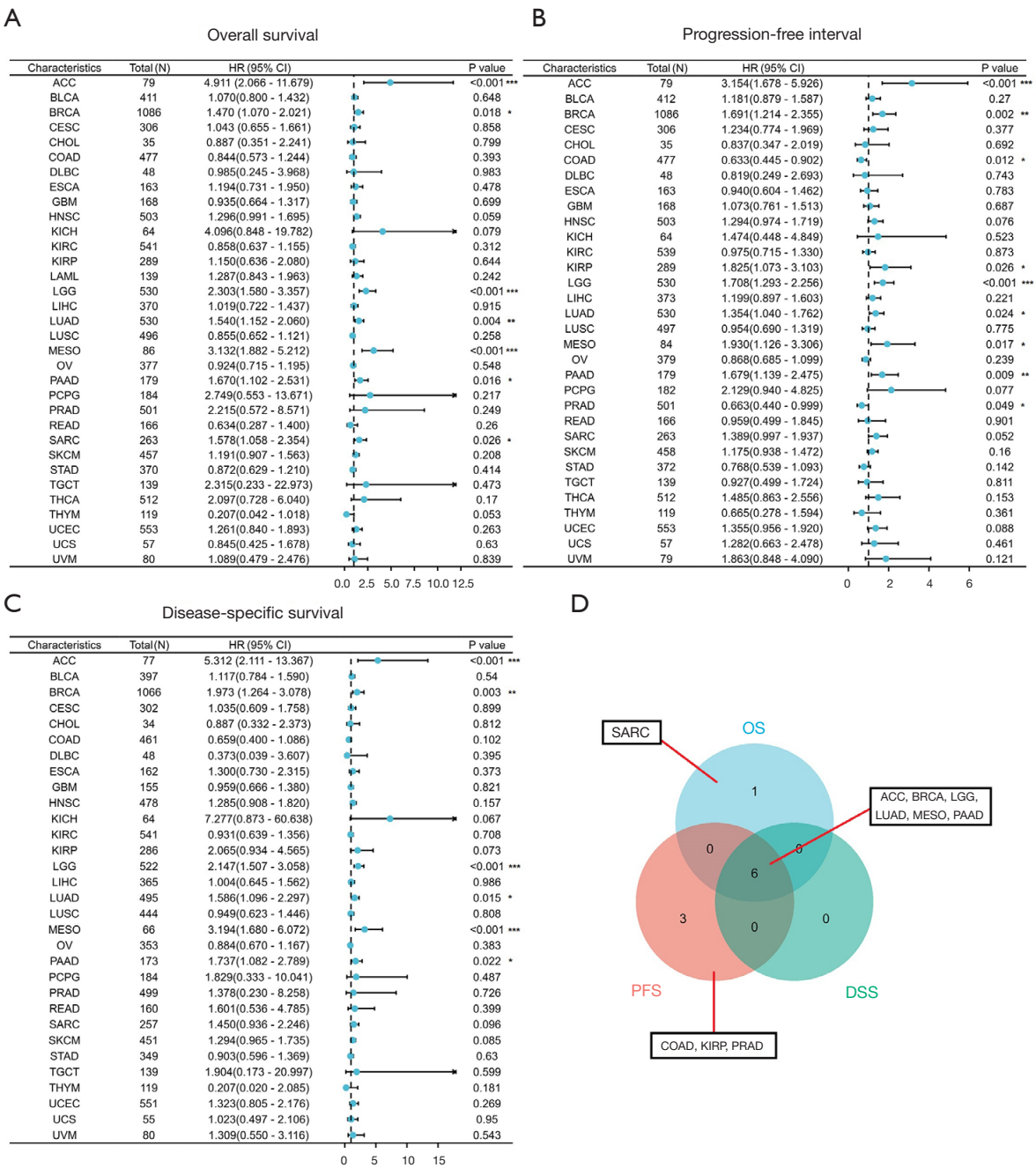

Figure 4 The connection between CENPN expression and cancer patient's prognosis. (A-C) Connection between CENPN expression and OS, PFI and DSS in cancer patients. (D) The Venn diagram illustrates the overlapping between OS, DSS, and PFS for various malignancies. *, P<0.05; **, P<0.01; ***, P<0.001. CI, confidential interval; DSS, disease-specific survival; HR, hazard ratio; OS, overall survival; PFI, progression-free interval; PFS, progression-free survival.

1.68–5.93), BRCA (HR =1.69, 95% CI: 1.21–2.36), KIRP (HR =1.83, 95% CI: 1.07–3.10), LGG (HR =1.71, 95% CI: 1.29–2.26), LUAD (HR =1.35, 95% CI: 1.04–1.76), The disadvantages of shorter PFS in patients with MESO (HR =1.93, 95% CI: 1.13–3.31) and PAAD (HR =1.68, 95% CI: 1.14–2.48); in patients with COAD (HR =0.63, 95% CI: 0.45–0.90) and PRAD (HR =0.66, 95% CI: 0.44–0.99), high *CENPN* expression was a favorable factor for longer

© AME Publishing Company.

PFS (*Figure 4B*). Similarly, high *CENPN* expression was linked to ACC (HR =5.31, 95% CI: 2.11–13.37), BRCA (HR =1.97, 95% CI: 1.26–3.08), LGG (HR =2.15, 95% CI: 1.51–3.06), LUAD (HR =1.59, 95% CI: 1.10–2.30). Risk factors for shorter DSS in patients with MESO (HR =3.19, 95% CI: 1.68–6.07) and PAAD (HR =1.74, 95% CI: 1.08–2.79) (P<0.05; *Figure 4C* and Figure S1C). The outcomes of the Venn diagram demonstrated that *CENPN* affected three prognostic indicators (OS, DSS, and PFS) in six types of patients, including ACC, BRAC, LGG, LUAD, MESO, and PAAD, suggesting that *CENPN* involved in affecting these cancers prognosis (*Figure 4D*).

We further analyzed the diagnostic value of CENPN in pan-cancer, as displayed in *Figure 5A*, and found that CENPN was effective in CESC (AUC =0.996), CHOL (AUC =0.914), COAD (AUC =0.956), ESCA (AUC =0.924), HNSC (AUC =0.930), LUSC (AUC =0.978), SARC (AUC =0.935), and STAD (AUC =0.951), UCEC (AUC =0.903) and other tumors (AUC >0.9). Moreover, CENPN has certain diagnostic potential (AUC >0.7) in the following tumors, including BLCA (AUC =0.763), BRCA (AUC =0.810), GBM (AUC =0.821), LIHC (AUC =0.843), LUAD (AUC =0.798), PAAD (AUC =0.754), PRAD (AUC =0.755), and READ (AUC =0.878) (*Figure 5B*). Overall, CENPN has a moderate-to-strong ability to distinguish between most cancers and healthy tissues.

CENPN Operates as an independent variable in some malignancies prognosis

To ascertain the risk factors affecting OS in cancer patients, we applied univariate and multivariate Cox regression analyses for five forms of cancer: ACC, BRCA, LGG, LUAD, and PAAD. The main treatment outcome for ACC [partial response (PR)/complete response (CR), HR =0.130, P=0.005] (*Figure 6A*, Table S1). The independent predictors for BRCA were N stage (N1 and N2 and N3, HR =1.689, P=0.02), M stage (M1, HR =2.171, P=0.03), clinical stage (stage III and IV HR =1.750, P=0.04), age (age >60 years, HR =2.205, P<0.001), and elevated *CENPN* expression (HR =1.546, P=0.02) (*Figure 6B*, Table S2). The primary treatment impact (PR/CR, HR =0.225, P<0.001), WHO grade (G3 stage, HR =2.782, P<0.001), and age (>40 years, HR =2.708, P<0.001) were independent predictors for LGG (*Figure 6C*, Table S3). The key treatment implication (PR/CR, HR =0.378, P<0.001) and N stage (N1 and N2 and N3, HR =1.646, P=0.03) were independent predictors for LUAD (*Figure 6D*, Table S4). In PAAD disease, the primary treatment outcome (PR/CR, HR =0.444, P<0.001) was found to be the only independent predictor variable (*Figure 6E*, Table S5).

We used components with P values below 0.1 in the univariate Cox regression analysis to create projected nomograms and calibration plots. We found that the nomogram' C-index was 0.866 (0.836–0.896) for ACC (*Figure 6F*), 0.724 (0.699–0.748) for BRCA (*Figure 6G*), 0.797 (0.775–0.820) for LGG (*Figure 6H*), 0.706 (0.678–0.734) for LUAD (*Figure 6I*), and 0.651 (0.614–0.688) for PAAD (*Figure 6J*). Afterward, we adjusted each nomogram to evaluate the dependability of the model. *Figure 6F-6J* show that the ideal spectral line is closely approximated by the calibration curves for the five cancer types. Thus, *CENPN* may be used to forecast patient outcomes for these cancers independently.

CENPN DNA methylation analysis

M6A methylation is vital for carcinogenesis and development. We ascertained the link between *CENPN* mRNA expression and m6A methylation modification levels in some tumors (*Figure 7A*). A total of 24 basic m6A methylation sites were selected: 10 writers (*CBLL1*, *METTL14/3*, *RBM15/15B*, *TRMT6*, *TRMT61A/B*, *WTAP*, and *ZC3H13*); three cleaners (*FTO*, *ALKBH3*, and *ALKBH5*) and 11 readers (*HNRNPA2B1*, *HNRNPC*, *IGF2BP1/2/3*, *RBMX*, *YTHDC1/2*, and *YTHDF1/2/3*). Heatmaps found that the *CENPN* expression had a favorable connection with many m6A methylation regulator expressions in different types of malignancies. Furthermore, we compared the *CENPN* promoter methylation level between healthy and tumor tissues. In comparison to healthy tissues, the *CENPN* promoter exhibited hypomethylation in BLCA, BRCA, CESC, COAD, HNSC, LIHC, LUAD, LUSC, PRAD, READ, SARC, testicular germ cell tumors (TGCT), and UCEC (*Figure 7B-7N*).

We focused on the relationship between *CENPN* methylation patterns and *CENPN* mRNA expression, as well as its influence on the cancer patient's prognosis, utilizing the GSCA database. In several cancers, with the exception of kidney chromophobe (KICH), UCEC, KIRP, KIRC, and thymoma (THYM), there was an inverse connection between *CENPN* methylation levels and *CENPN* mRNA expression (Figure S2A). Moreover, we found that *CENPN* hypomethylation levels may be associated

© AME Publishing Company.

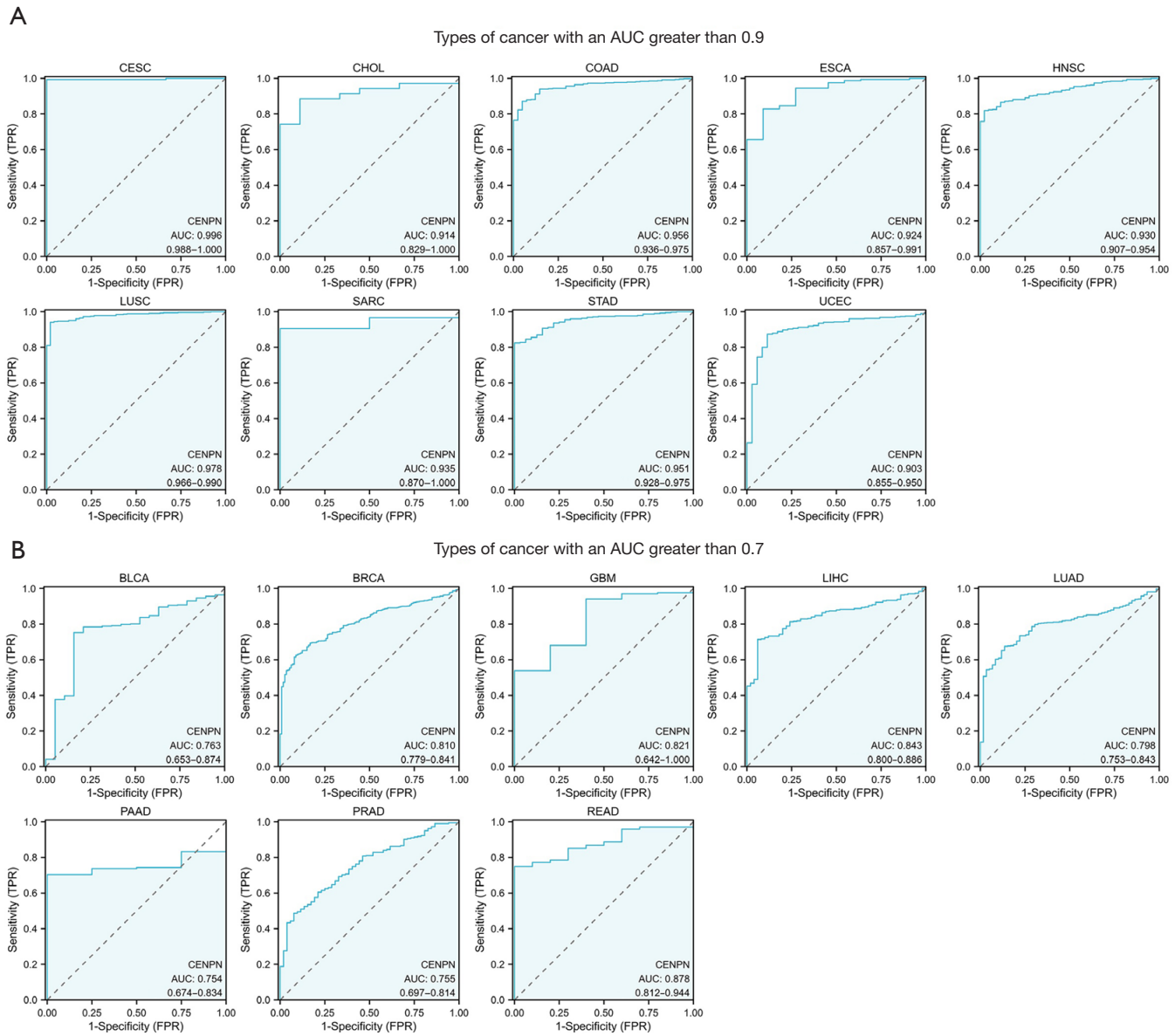

Figure 5 ROC curves of CENPN expression in pan-carcinoma. (A) CENPN expresses malignancies with a high diagnostic significance (AUC >0.9), encompassing CESC, CHOL, COAD, ESCA, HNSC, LUSC, SARC, STAD, and UCEC. (B) CENPN expresses cancer with many diagnostic significances (AUC >0.7), encompassing BLCA, BRCA, GBM, LIHC, LUAD, PAAD, PRAD, and READ. Values below the AUC represent the corresponding 95% CI. AUC, area under the curve; CI, confidence interval; FPR, false positive rate; ROC, receiver operating characteristic; TPR, true positive rate.

with a worse prognosis in cancer patients (Figure S2B). Additionally, the low methylation level of *CENPN* was an undesirable variable affecting the LGG patient's prognosis (Figure S2C).

In summary, in most cancers, the *CENPN* promoter exhibited hypomethylation and affected patient prognosis.

Relationship between CENPN expression and genetic alteration

Through genetic research, we explored whether *CENPN* could be applied as a target for molecular therapeutics. We found that 156 out of 10,443 specimens (1.5%) showed *CENPN* mutations, with deep deletion being the prevailing

© AME Publishing Company.

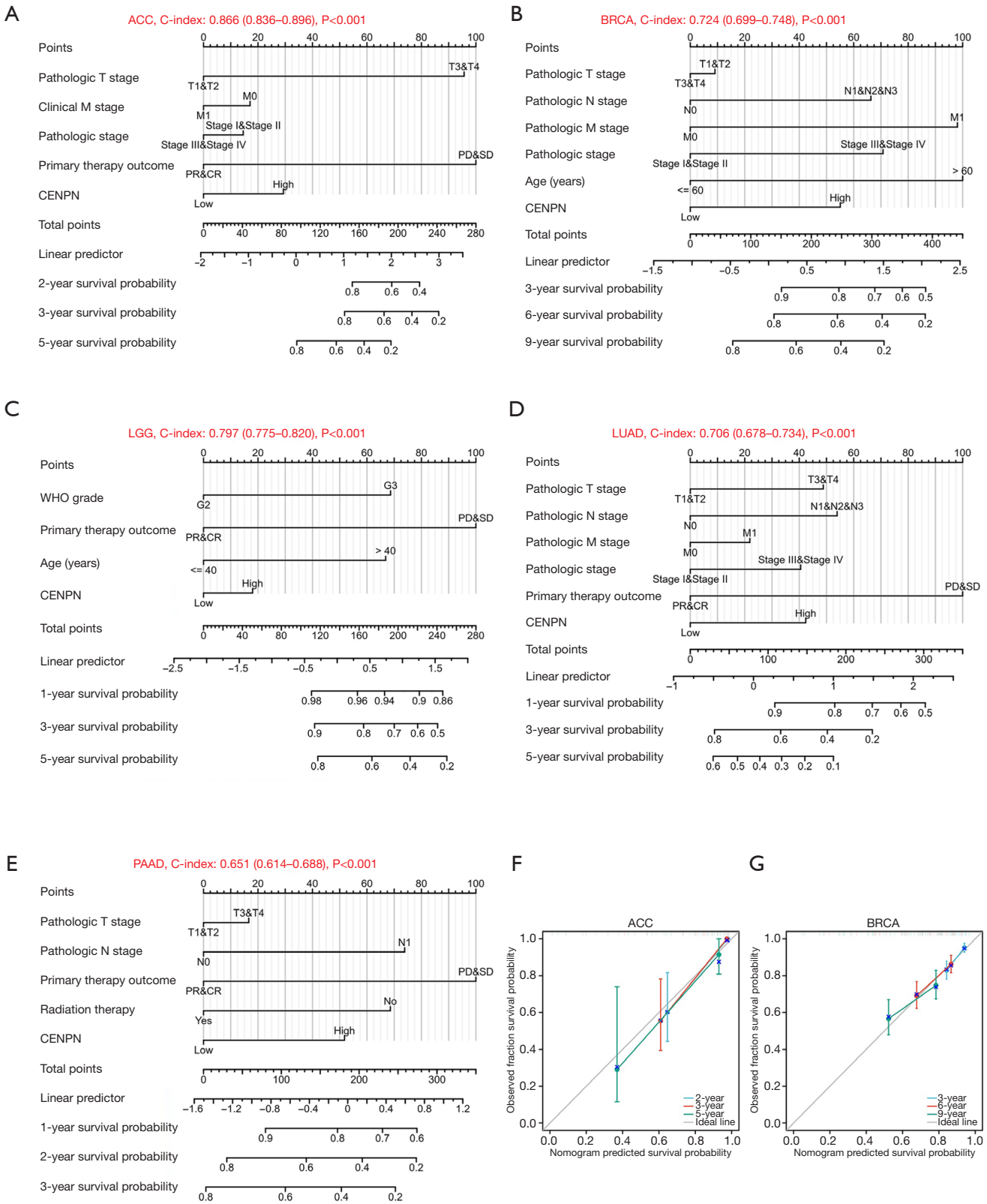

© AME Publishing Company.

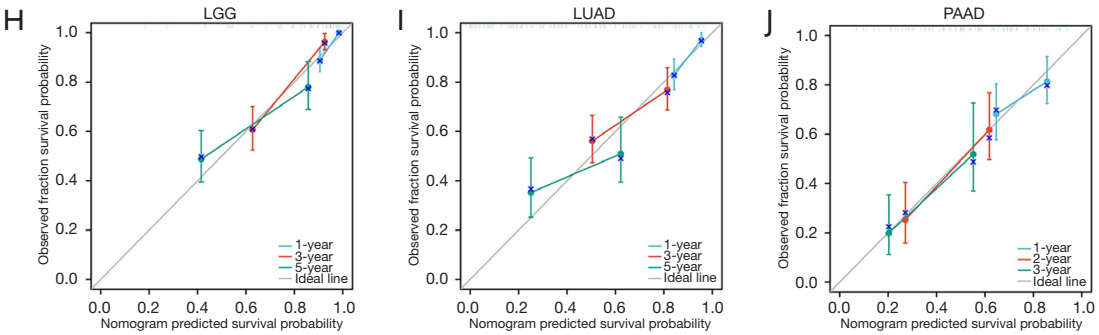

Figure 6 Nomograms and calibration curves predict patient OS in five malignancies. Nomograms of (A) ACC; (B) BRCA; (C) LGG; (D) LUAD; (E) PAAD. Calibration curves of (F) ACC, (G) BRCA, (H) LGG, (I) LUAD, and (J) PAAD. The horizontal and vertical coordinates correspond to the anticipated and found survival probabilities of the model, respectively. The accuracy of the model increases as each curve approaches the ideal line, indicating closer agreement between predicted and actual outcomes. CR, complete response; OS, overall survival; PR, partial response; PD, progressive disease; SD, stable disease.

in *CENPN* (*Figure 8A*). Missense mutation and synonymous substitutions possessed 45.36% and 19.20% of all mutations, respectively (Figure S3A). In contrast, rare homozygous amplification occurred mainly in KIRP, ACC and KICH (Figure S3B). Moreover, the most dominant CNV category was C>T (31.58%), followed by G>A (16.37%) (Figure S3C). The greatest mutation frequency was found in these five cancer types: PRAD (4.86%), UCEC (4.45%), BLCA (3.41%), COAD (2.29%), and BRCA (2.25%) (*Figure 8B*). *S107L* was the largest mutation site in the *CENPN* domain, which occurred in three patients with COAD, three patients with UCEC, one patient with GBM, and one SKCM patient (*Figure 8C*). We demonstrated it in the CENPN protein three-dimensional structure (*Figure 8D*).

Then, we implemented the GSCA database to investigate the connection between *CENPN* mutations and *CENPN* mRNA expression, as well as the prognostic implications for cancer patients. CNV mutations in the *CENPN* gene were shown to possess a negative implication on the patient's prognosis with COAD, ESCA, KICH, KIBP, PCPG, UCEC, and UVM (*Figure 8E*). The CNV pie chart results showed that homozygous and heterozygous amplifications were present in most cancers. In KIBP and ACC, we found that the mutations were mostly homozygous amplification, while homozygous deletion was mostly found in SKCM, LUSC, UCEC, TGCT, LIHC, PRAD, SARC, BRCA, uterine carcinosarcoma (UCS), OV and other cancers. Furthermore, *CENPN* mutations were positively linked to *CENPN* mRNA expression in patients with KIRP, SARC, PAAD, READ, LUAD, KIRC, GBM, STAD, HNSC, UCS, OV, LIHC, ESCA, CESC, BLCA, SKCM, LISC, and BRCA (Figure S3D). The majority of malignancies have genetic alterations in the *CENPN* gene that are implicated in the cancer patient's prognosis.

The connection between CENPN expression and immune infiltration and immune response

TMB, MSI, and NEO can predict the response status of cancer patients to immunotherapy and are considered to be tumor immunotherapy response predictors. Therefore, we initially investigated the connection between the *CENPN* mRNA expression levels and the variables TMB, MSI, and NEO. The radar chart emerged that there were significant variations in ACC (R=0.48), STAD (R=0.41), BRCA (R=0.41), lymphoid neoplasm diffuse large B-cell lymphoma (DLBC) (R=0.39), SARC (R=0.39), PAAD (R=0.34), LGG (R=0.27), UCEC (R=0.25), BLCA (R=0.20), COAD (R=0.14), LUSC (R=0.13), OV (R=0.12), and HNSC (R=0.11) and other 13 cancer types, the *CENPN* mRNA expression level had a positive link to TMB. The TMB demonstrated a negative relationship with THCA (R=−0.11) and THYM (R=−0.63) (P<0.05; *Figure 9A*). Next, *CENPN* mRNA expression exhibited a positive connection with MSI in seven cancer types, encompassing SARC (R=0.29), KICH (R=0.28), STAD (R=0.27), MESO (R=0.25), PAAD (R=0.25), LIHC and BRCA (R=−0.02). The MSI was adversely connected with THCA (R=−0.15) (P<0.05; *Figure 9B*). Similarly, *CENPN* mRNA expression found a positive link with NEO in DLBC (R=0.43), UCEC (R=0.18), LUAD (R=0.15), and BRCA (R=0.13) (*Figure 9C*).

Moreover, we ascertained the connection between

© AME Publishing Company.

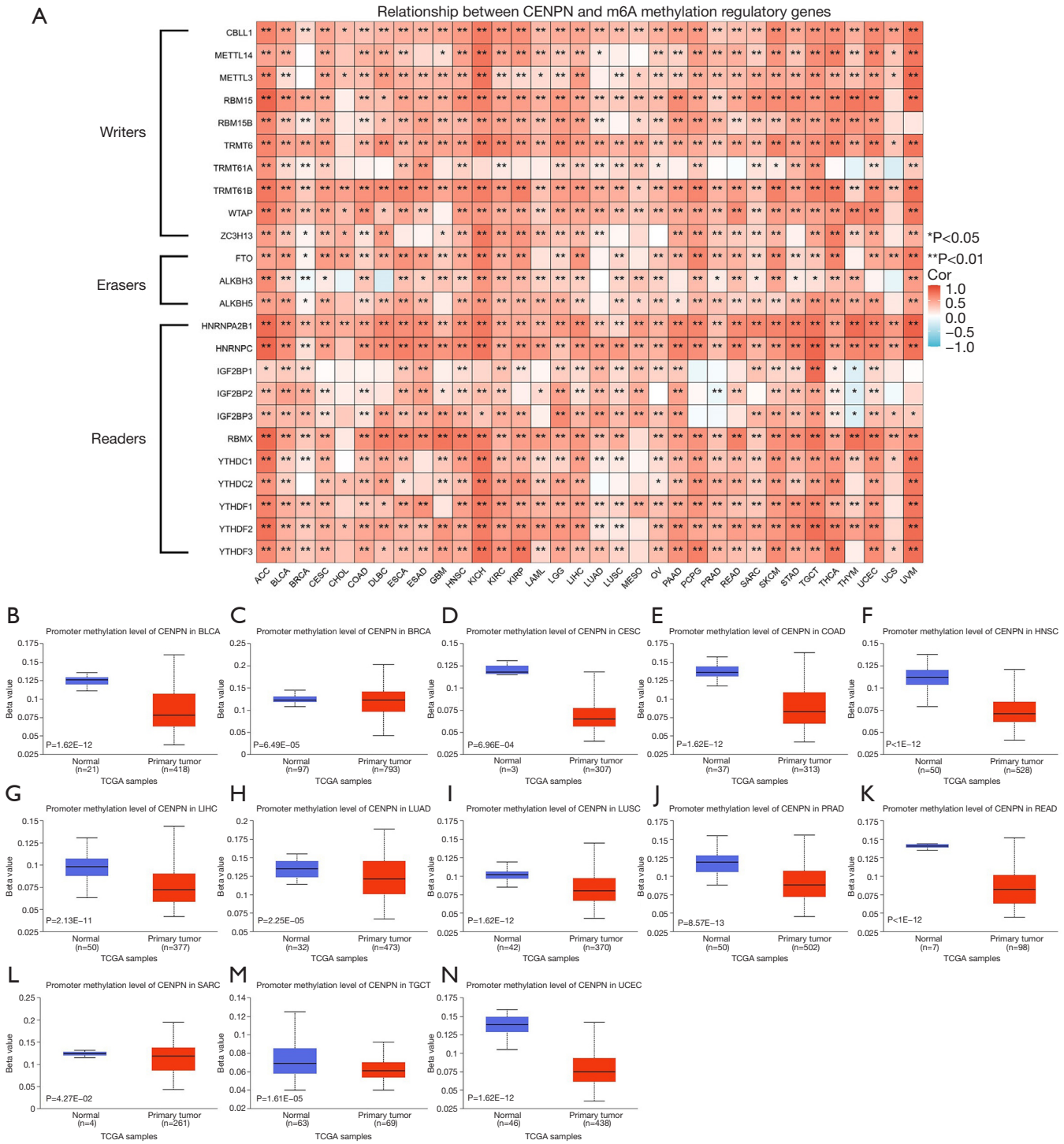

Figure 7 CENPN epigenetic methylation analysis. (A) The relationship between the CENPN mRNA expression and the regulatory variables of m6A methylation in various types of cancer. Differential promoter methylation levels (beta values) of CENPN in normal tissues and malignancies, as determined by UALCAN, encompassing (B) BLCA, (C) BRCA, (D) CESC, (E) COAD, (F) HNSC, (G) LIHC, (H) LUAD, (I) LUSC, (J) PRAD, (K) READ, (L) SARC, (M) TGCT, and (N) UCEC. mRNA, messenger RNA; TCGA, The Cancer Genome Atlas; UALCAN, The University of Alabama at Birmingham Cancer Data Analysis Portal.

© AME Publishing Company.

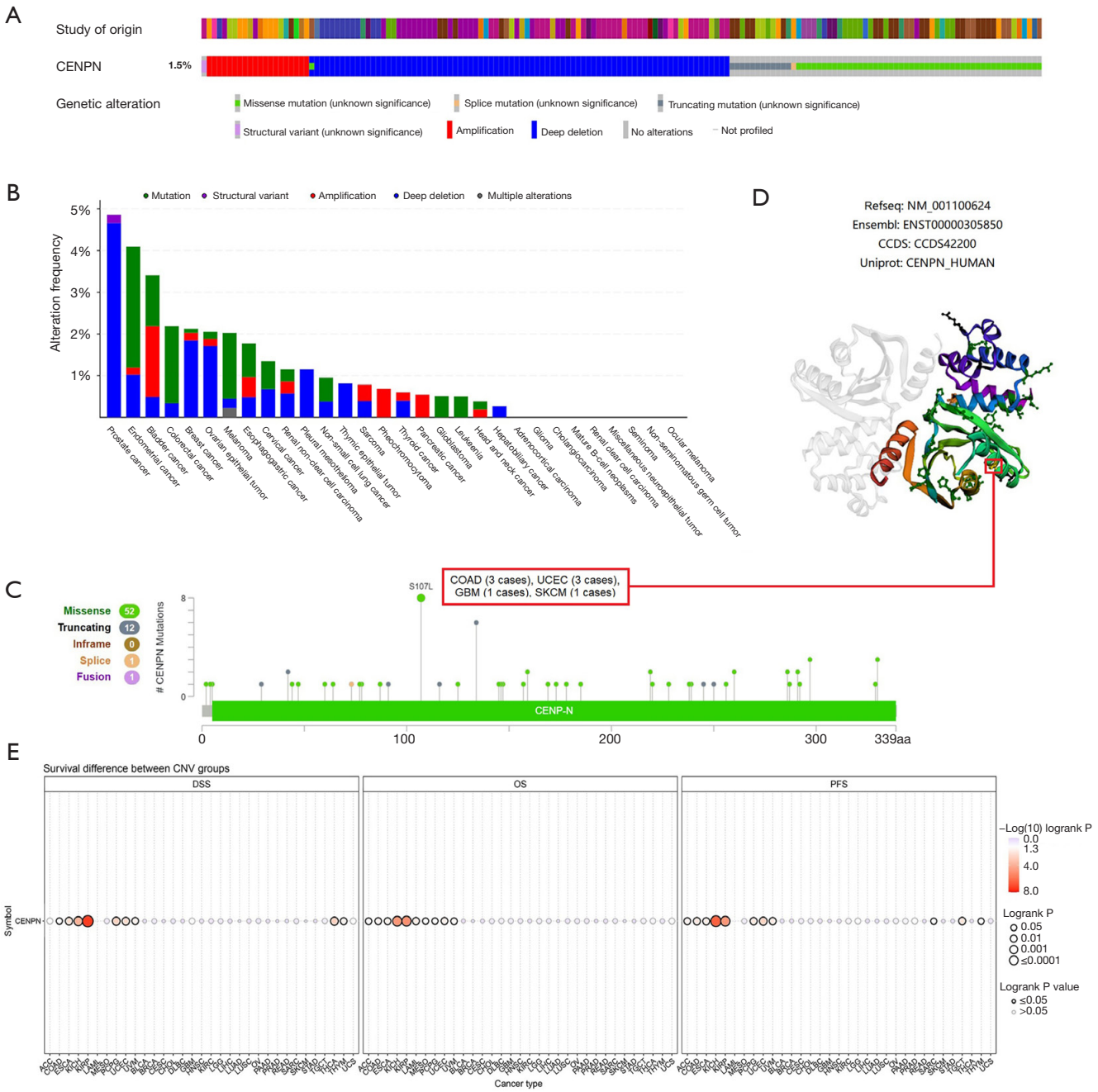

Figure 8 Mutated characteristics of CENPN in various tumors. (A) Alterations summary in CENPN expression in various tumors. (B) Bar chart displaying the prevalence and kinds of alterations in the CENPN across various forms of cancer. (C) The CENPN mutation landscape with the location, types, and quantity and their connection with protein domains. (D) The protein 3D structure depicts several CENPN mutations. (E) The connection between CNV in CENPN and cancer patient's prognosis. CNV, copy number variants; CCDS, consensus coding sequence; DSS, disease-specific survival; OS, overall survival; PFS, progression-free survival.

© AME Publishing Company.

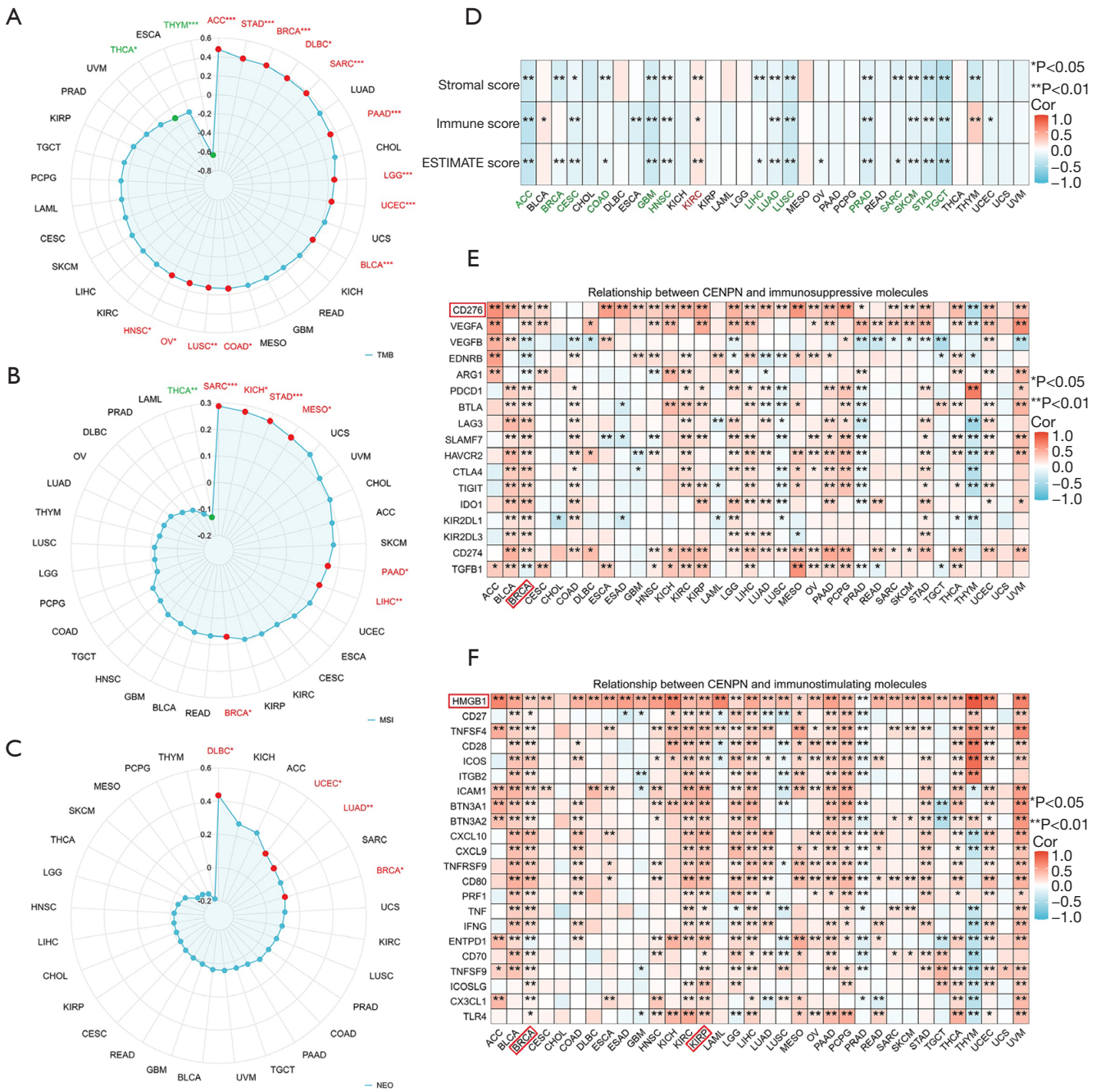

Figure 9 CENPN expression is linked to TMB, MSI, NEO, TME, and immunological checkpoints in 33 cancer types. Connection between CENPN expression and (A) TMB, (B) MSI, (C) NEO, (D) Stromal Score, Immune Score, ESTIMATE Score, (E) immunosuppressive molecules expression, and (F) immunostimulating molecules in 33 cancers. *, P<0.05; **, P<0.01. MSI, microsatellite instability; NEO, neocancer antigen; TMB, tumor mutational burden; TME, tumor microenvironment.

© AME Publishing Company.

CENPN mRNA expression levels and scores related to tumor stromal, immune invasion, and tumor purity in pan-cancer. The heat map revealed a negative link between the *CENPN* mRNA expression level and the scores for tumor stromal, immune invasion, and tumor purity in 14 different kinds of cancer, encompassing ACC, BRCA, CESC, COAD, GBM, HNSC, LIHC, LUAD, LUSC, PRAD, SARC, SKCM, STAD, and TGCT (P<0.05; *Figure 9D*). Conversely, in KIRC, *CENPN* expression emerged with a positive connection with scores indicating tumor stromal, immunological invasion, and tumor purity (P<0.05).

Moreover, we determined the link between *CENPN* and immune checkpoints. In various cancers, encompassing BLCA, BRCA, LGG, LIHC, PAAD, PCPG, READ, and UVM, the *CENPN* expression was favorably correlated with multiple immune checkpoint expressions (*Figure 9E*). We conducted a thorough assessment of the connection between *CENPN* expression and immune checkpoint inhibitors (ICIs). We found that *CENPN* expression was shown to be favorably associated with numerous ICIs in BLCA, BRCA, COAD, KIRC, KIRP, LGG, LIHC, OV, PAAD, PCPG, PRAD, STAD, THCA, USC, and UVM. BRCA demonstrated a significant positive association with almost every ICI, and the ICI *CD276* was expressed in almost all cancers. Similarly, we selected 22 immune checkpoint activators to study the link between *CENPN* expressions. In most cancers, the *CENPN* expression found a positive connection with checkpoint activators, exclusively the immune checkpoint activator *HMGB1*. For BRCA and KIRP, most immune checkpoint activators were positively linked to *CENPN* expression (*Figure 9F*). In general, the *CENPN* expression was significantly connected with immunological checkpoints in the majority of malignancies.

Tumor-infiltrating immune cells (TIICs) contribute to the tumor microenvironment (TME) and possess a strong correlation with tumor aggressiveness. We applied the ssGSEA technique to ascertain the connection between the *CENPN* mRNA expression and the 24 TIICs infiltration levels. The heatmap analysis exhibited that the *CENPN* mRNA expression level had an adverse connection with the invasiveness of the majority of TIICs in seven different forms of cancer, namely ACC, GBM, LUSC, SKCM, STAD, TGCT, and UCEC. In contrast, Th2 found a strong positive relationship with the *CENPN* mRNA expression level in many cancer cases (*Figure 10A*). We ascertained the link between *CENPN* mRNA expression levels and the various types of TIICs infiltration using the TIDE method and the Timer 2.0 database. The findings showed a favorable connection between the *CENPN* mRNA expression level and the myeloid-derived suppressor cells (MDSCs) infiltration level from the bone marrow in different cancer types. There was a favorable connection between the *CENPN* mRNA expression level and the MDSC infiltration levels in eight distinct kinds of cancer, namely ACC (R=0.760), ESCA (R=0.554), LGG (R=0.529), LIHC (R=0.517), LUAD (R=0.627), PAAD (R=0.547), READ (R=0.553), and UCEC (R=0.522) (P<0.05; *Figure 10B*).

Protein-protein interaction (PPI), GO, KEGG, and GSEA of CENPN-linked Genes

To get a comprehensive understanding of the *CENPN* molecular pathways involved in tumor initiation and establishment, we conducted enrichment experiments to investigate the *CENPN*-coexpressed genes. We acquired the first 100 *CENPN* co-expressed genes (Table S6) from the Gene Expression Profiling Interactive Analysis 2 (GEPIA2) database. The STRING tool was applied to examine 50 adjacent nodes of the *CENPN* gene network, and a PPI network diagram was built (*Figure 11A*). The Venn diagram exhibited that there are five common genes, *CENPA*, *CENPH*, *CENPI*, *CENPL*, and *CENPO*, and we can consider that these five common genes are the most strongly associated with *CENPN* (*Figure 11B*) and visualize the correlation (*Figure 11C*). Moreover, we explored the expression of these five common genes in pancarcinoma (*Figure 11D*). Afterward, typically, 100 genes that were co-expressed with *CENPN* and 50 proteins that were bound to *CENPN* were chosen for functional enrichment analysis. Moreover, it was found that besides the 10 KEGG pathways, there were 333 GO classes, including 261 biological processes (BPs), 46 cellular components (CCs), and 26 molecular functions (MFs) (the supplementary table is available at https://cdn.amegroups.cn/static/public/tcr-24-1291-1.xlsx). We displayed the first three cancer-associated elements inside every GO entry. The GO analysis revealed that *CENPN* mostly participated in BP related to protein genomics, organelle fission, and nuclear division (*Figure 11E*). Together, they participate in the composition of CC, such as chromosomal region, chromosomal, centromere regions, and DNA packaging complex (*Figure 11F*). Moreover, the MF contained protein heterodimerization activity, microtubule binding, and tubulin binding (*Figure 11G*). The KEGG analysis showed that *CENPN* mainly mediated neutrophil extracellular

© AME Publishing Company.

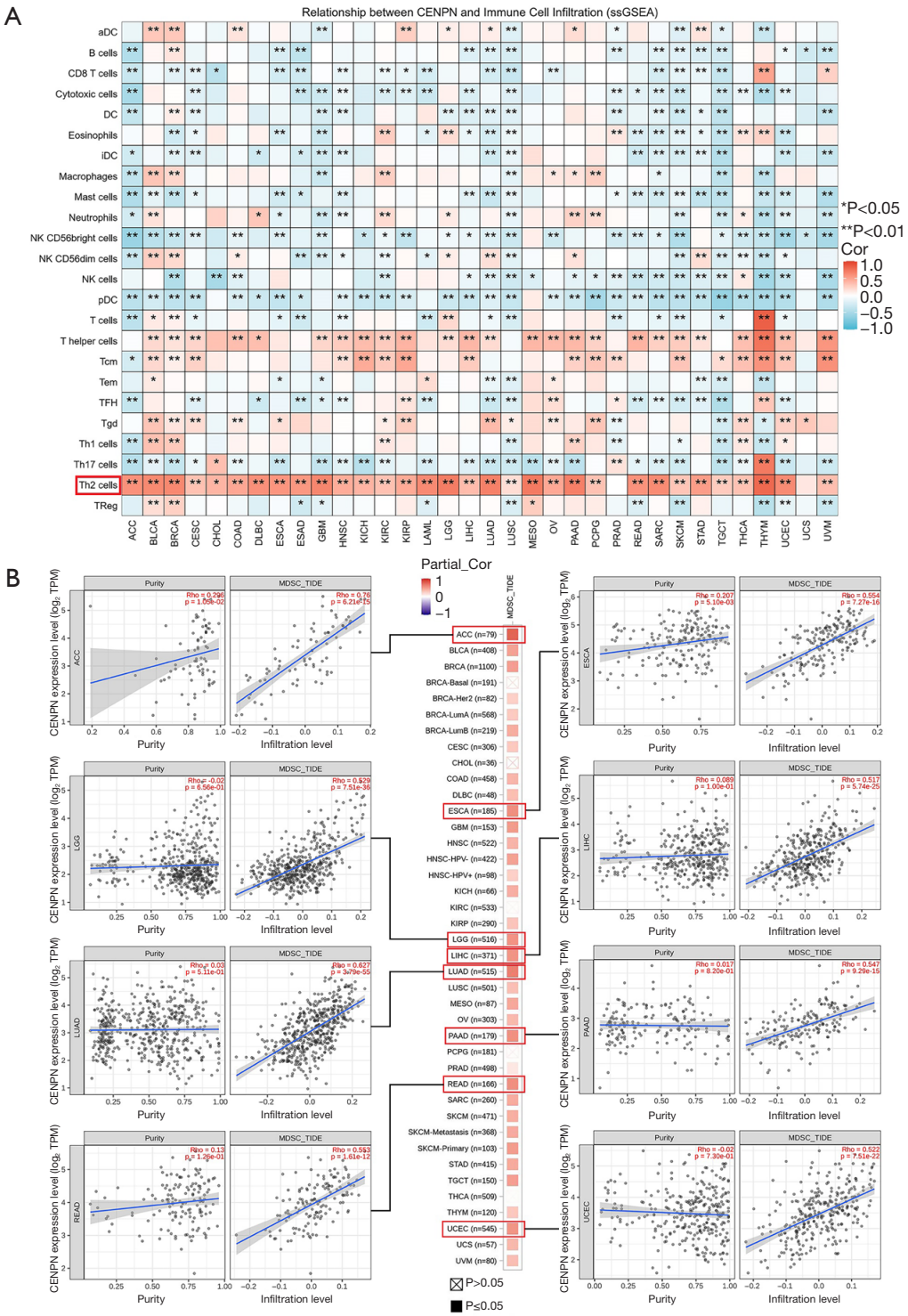

Figure 10 Correlations between immune cell infiltration levels and CENPN expression in pan-cancer. (A) The link of CENPN expression and immune infiltration with the ssGSEA method. (B) CENPN expression connections analysis with CAF cells immune infiltration according to TIMER 2.0 database, scatter plots encompassing ACC, ESCA, LGG, LIHC, LUAD, PAAD, READ and UCEC. CAF, Cancer-associated fibroblasts; HPV, human papillomavirus; MDSC, myeloid-derived suppressor cell; ssGSEA, single-sample Gene Set Enrichment Analysis; TIMER, Tumor Immune Estimation Resource; TPM, transcripts per million; TIDE, Tumor Immune Dysfunction and Exclusion.

© AME Publishing Company.

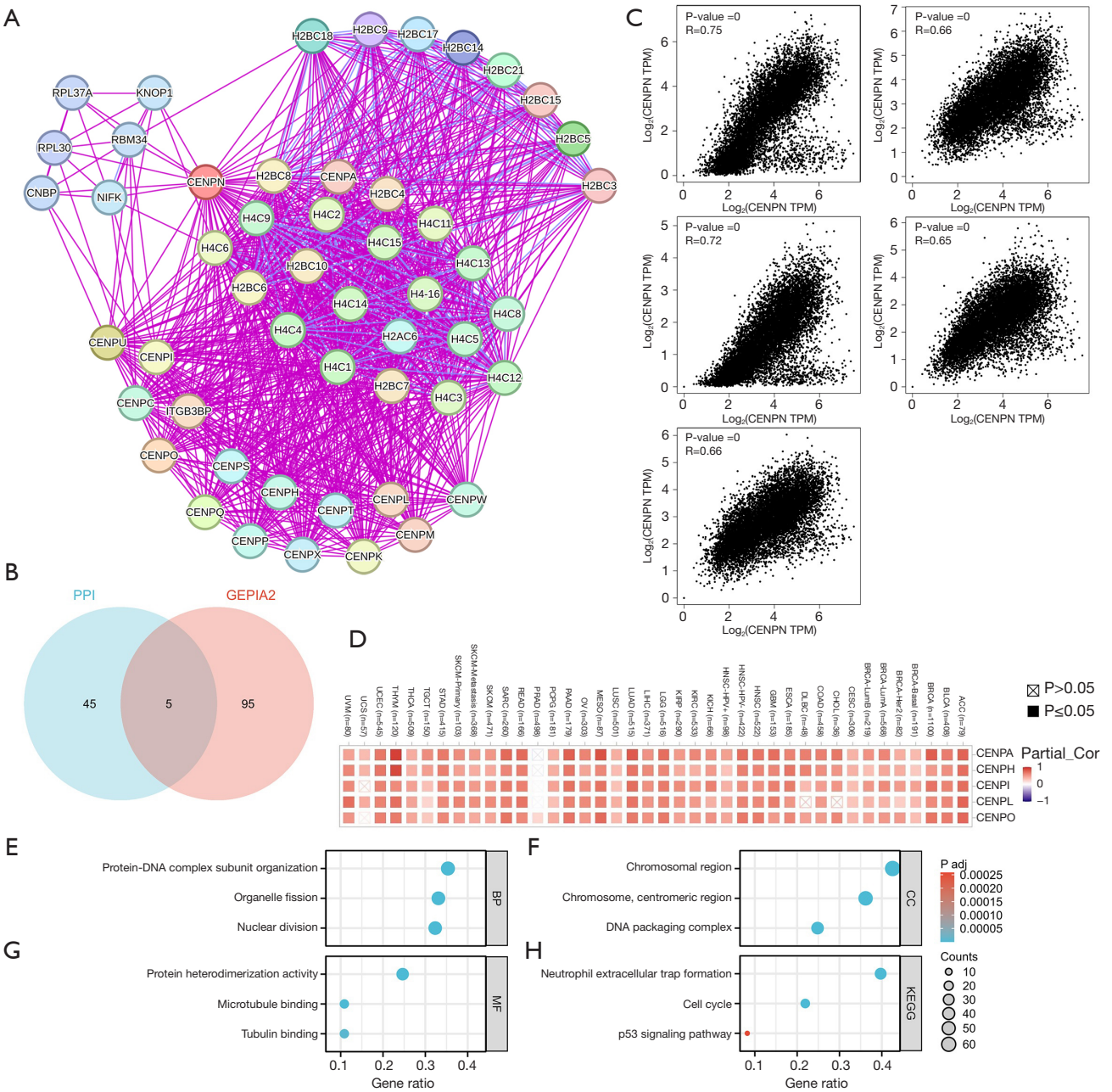

Figure 11 Analysis of CENPN-linked genes, including interacting proteins and functional enrichment. (A) PPI Network for CENPN. (B) The Venn diagram analysis of the overlapping of CENPN-binding and interacting genes following selection. (C) Five common genes were associated with CENPN. (D) Relationship between five common genes in 33 cancers. GO analyses, including (E) BP, (F) CC, (G) MF and (H) KEGG pathway. BP, biological pathways; CENPN, centromere protein N; CC, cellular component; GO, Gene Ontology; KEGG, Kyoto Encyclopedia of Genes and Genomes; MF, molecular function; PPI, protein-protein interaction; TPM, transcripts per million.

trap formation, cell cycle, and p53 pathway in cancer (*Figure 11H*).

To investigate the potential processes by which *CENPN* contributed to pan-cancer, we executed a GSEA using the Respondome Pathway Database. Six cancers, ACC, BRCA, LGG, LUAD, MESO, and PAAD, which were negatively correlated with *CENPN* expression in prognosis, were selected, and the results showed that the genes that emerged

© AME Publishing Company.

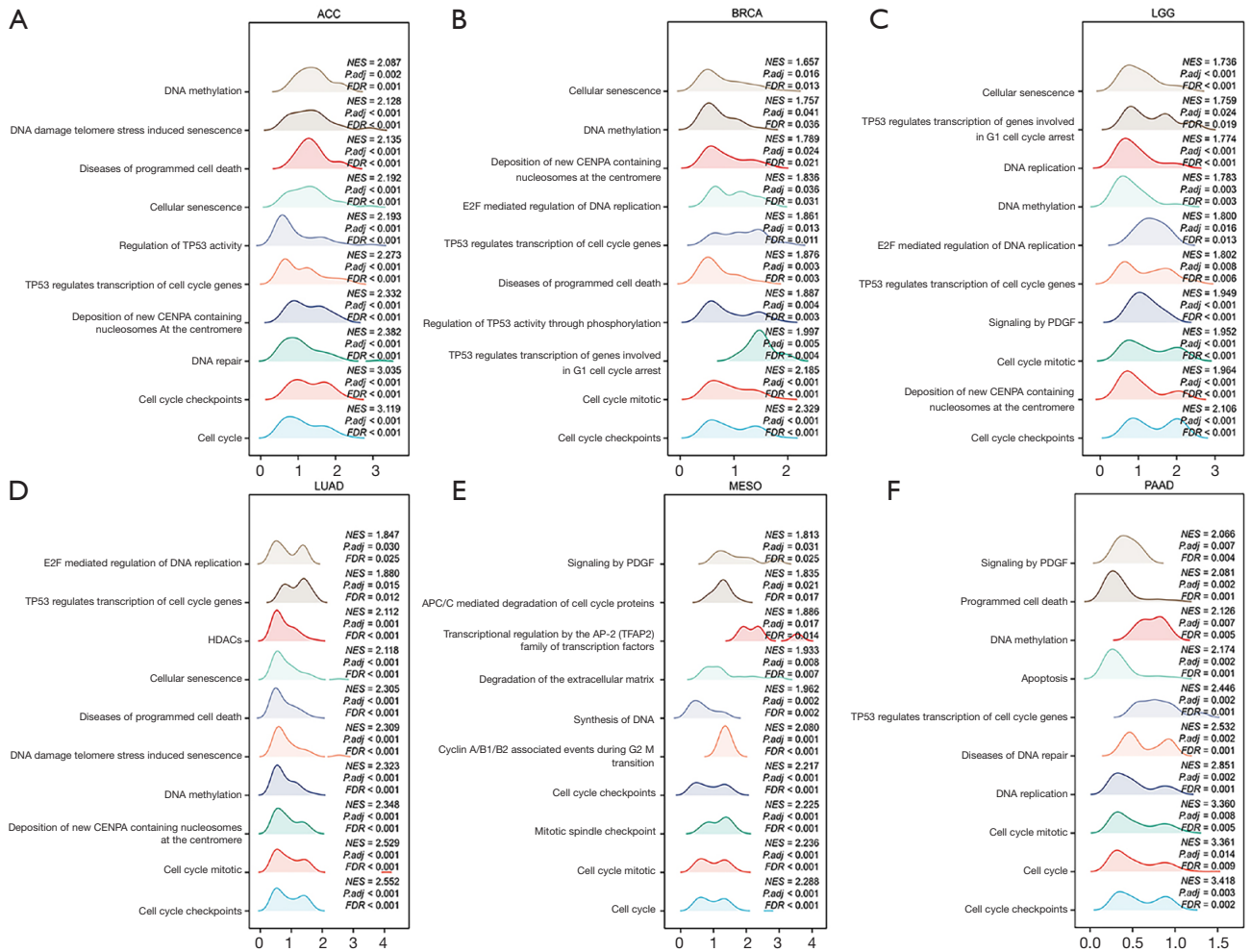

Figure 12 GSEA functional enrichment analysis of CENPN in six cancers. The initial 10 reaction pathways were linked to CENPN expression in (A) ACC, (B) BRCA, (C) LGG, (D) LUAD, (E) MESO, and (F) PAAD. FDR, false discovery rate; GSEA, Gene Set Cancer Analysis; NES, normalized enrichment score; PDGF, platelet-derived growth factor.

a positive connection with *CENPN* expression were mostly enriched in DNA methylation, the cell cycle, and the TP53 pathway (*Figure 12A-12F*). In summary, we deduced that *CENPN* had an essential involvement in cancer by regulating DNA methylation and affecting biological functions like the TP53 pathway.

To verify the phenotypic regulatory function of CENPN in BC cells

To examine the *CENPN* function in BC cells, we created vectors that overexpressed *CENPN* and introduced them into the MDA-MB-231 human BC cell line using transfection. The efficacy of *CENPN* overexpression was verified using Western blot analysis (*Figure 13A*,*13B*).

To ascertain the correlation between *CENPN* and the growth of BC cells, we implemented the CCK-8 technique to estimate these cells' proliferation and viability. The introduction of small interfering *CENPN* (si-*CENPN*) into certain BC cell lines at multiple time intervals (0, 24, 48, and 72 h) led to a significant enhancement in cell proliferation and viability (*Figure 13C*). In addition, overexpression of *CENPN* emerged to inhibit apoptosis in BC cells (*Figure 13D*,*13E*). The *CENPN* implications on the chosen BC cell migration and invasion capacities were confirmed via further transwell and invasion assays. The outcomes found a significant rise in the BC cell's capacity to invade and migrate following the *CENPN* overexpression

© AME Publishing Company.

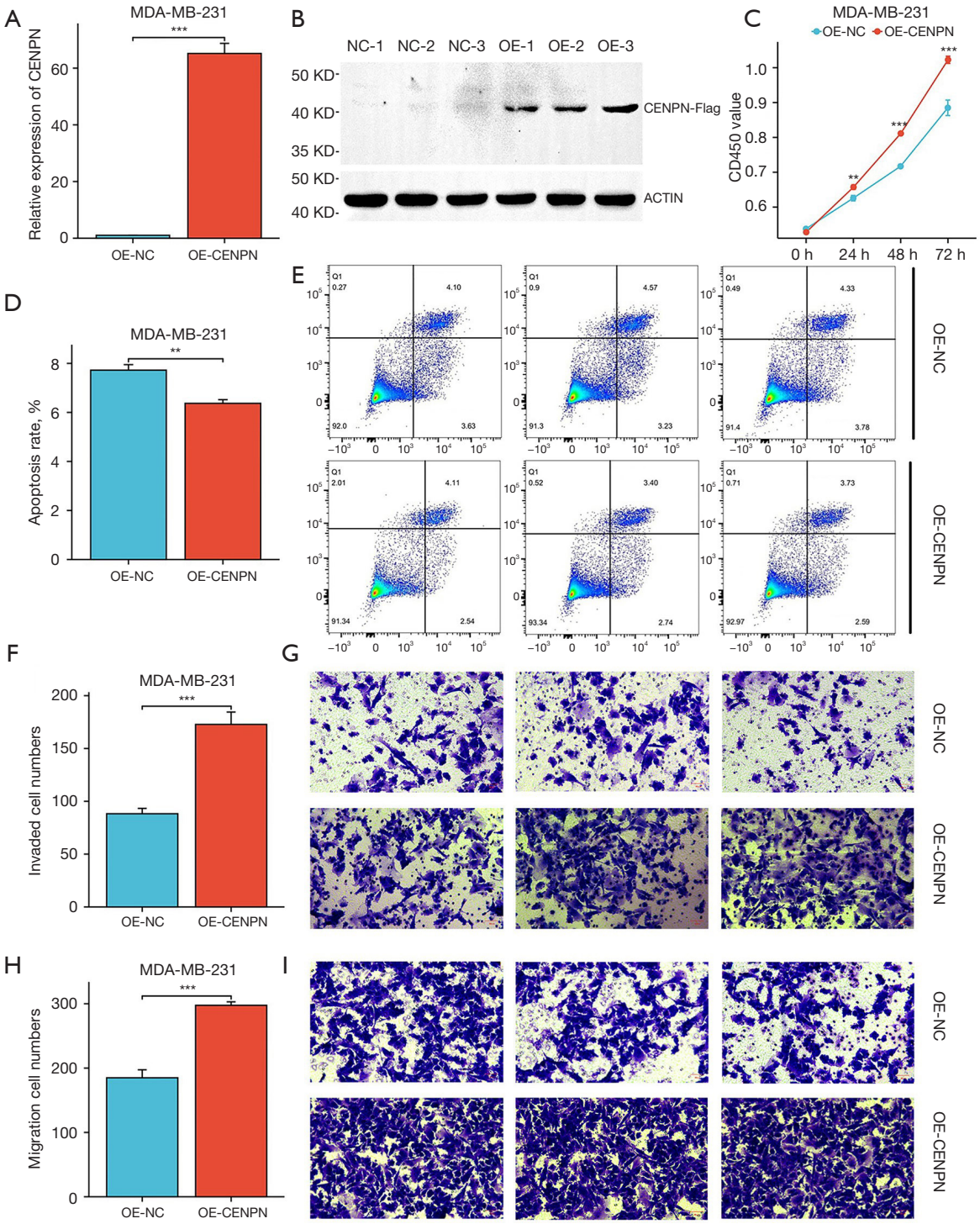

Figure 13 The phenotypic regulating function of CENPN in BC cells. (A,B) The expression efficiency of overexpressed CENPN in the MDA-MB-231 cell line was detected. (C) Overexpressed CENPN promoted the proliferation of BC cell lines. (D,E) Overexpressed CENPN inhibited the BC cell lines' apoptosis. (F,G) Overexpressed CENPN promoted the BC cell line invasion. (H,I) Overexpressed CENPN promoted the migration of BC cell line. *In vitro* migration assays were performed using transwell chambers (3422, Corning, USA). Stained with 0.1% crystal violet (C0121, Beyotime). The cells were observed and counted under inverted microscope (MF52-N, Mshot) at 200× magnification. **, P<0.01; ***, P<0.001. BC, breast cancer; NC, negative control; OE, over-expression.

© AME Publishing Company.

(*Figure 13F-13I*). Our work demonstrated that the upregulation of *CENPN* enhanced the BC cell's proliferation, invasion, and migration while suppressing the BC cell's apoptosis.

Discussion

CENPN, a member of the centromere protein family, contributes to cell mitosis by regulating centromere assembly and chromosome division through binding to chromosomes (20). Although *CENPN* has been found to contribute to a variety of cancer development, there is a lack of research results on *CENPN* in pan-cancer. Here, we use a multi-dataset-based bioinformatics approach to systematically elucidate the potential clinical function of *CENPN* in patients with multiple malignancies.

Our research showed that mRNA expression of *CENPN* was higher in various tumor tissues and correlates with poorer prognosis in patients, aligning with earlier studies (21,22). Our findings emerged, except that cancer tissues had a much lower *CENPN* expression level than corresponding normal tissues. Nevertheless, in several tumors, the *CENPN* expression level was significantly elevated compared to the nearby normal tissues. It is worth noting that in ACC, BRCA, KIRP, and LUAD, *CENPN* showed an increasing trend with the progression of tumor stage, which indicates that *CENPN* may be a marker leading to the poor prognosis of these cancers. Prior research has found that patients with the C3 subtype possess the worst tumor growth and the best prognosis compared to different immune subtypes (23). Our researchers found that *CENPN* had the lowest level of expression in the C3 immune subtype across several types of malignancies, which aligns with earlier research results. These findings indicate that *CENPN* exhibits significantly elevated levels of expression in the majority of malignant tumors and might potentially serve as a prognostic marker for poor prognosis.

Based on Cox and KM survival analysis, elevated *CENPN* expression was closely linked to poor OS, DSS, and PFS in tumor patients. Especially for patients who experienced ACC, BRAC, LGG, LUAD, MESO, and PAAD, the elevated *CENPN* expression affected the three prognostic indicators at the same time, suggesting that *CENPN* may be a key factor impacting the cancer's prognosis. Some prior studies have also verified that the *CENPN* expression could be a potential predictive indicator of reduced survival in some solid tumor patients (6-10), which is the same as the conclusion of our study. It has been further proved that *CENPN* may be a biomarker for detecting tumor survival and prognosis.

We also found that the elevated *CENPN* expression could be an independent factor impacting the tumor patients' prognosis. In ESCC, *CENPN* is involved as a feature gene in building an effective tool for predicting OS (10). Similarly, the construction of a survival prognosis model found that *CENPN* was identified as a separate LUAD risk factor and may be operated on to ascertain the LUAD patient's survival rate (24). Our study is the first to suggest that *CENPN* expression may be an independent predictor of BRCA.

We further studied the diagnostic significance of *CENPN* in pancarcinoma. Previous studies have found that *CENPN*'s diagnostic level in COAD and ESCA is superior to its common tumor biomarkers (10,25). We found similar outcomes in our investigation. Moreover, we found for the first time that *CENPN* showed great diagnostic value for CESC (AUC =0.996), but further sample experiments are still needed. In summary, *CENPN* is anticipated to emerge as a new diagnostic and predictive biomarker for a wide range of malignancies.

The occurrence of a tumor is usually strongly connected with the abnormal expression or change of genes, and the abnormal gene expression can be caused by gene amplification (26) or methylation status (27), thus accelerating the tumor process. We found that elevated *CENPN* expression was negatively linked to promoter methylation in most cancers. We have previously concluded that high *CENPN* expression is frequently connected with poorer patient outcomes. Therefore, we believe that the low methylation level of *CENPN* may be one of the factors resulting in a worse prognosis for cancer patients. Furthermore, we concluded that the epigenetic mechanism of *CENPN* may have a key function in the pan-cancer process. The primary factor contributing to cancer development is gene mutation, and the tumor prognosis may be predicted by identifying particular gene mutations. The CNV status of *CENPN* is often associated with elevated *CENPN* expression in the majority of cancer cases. This correlation possesses a detrimental implication on the patient's prognosis. We are the first to reveal the importance of *CENPN* mutation and methylation in pancarcinoma.

With the development of immunotherapy, immune checkpoint inhibitor (ICI) therapy has emerged to be one of the most promising and effective immunotherapies (28). TMB, MSI, and NEO can be operated as predictive biomarkers for tumor therapy (29), and higher TMB,

© AME Publishing Company.

MSI, and NEO imply better response to ICI and better prognosis (30). Hence, we estimated the connection between the *CENPN* expression levels and the variables TMB, MSI, NEO, and immunological checkpoints. Our investigation revealed a favorable connection between the *CENPN* expression in BRCA and the levels of TMB, MSI, and NEO. Furthermore, we exhibited a strong favorable connection between BRCA and almost all immunological checkpoint inhibitors, suggesting that *CENPN* could be a possible target for improving ICI efficacy in BRCA patients. Our study analyzed the link between *CENPN* and immunological checkpoint genes, and the outcomes found that *CENPN* may interact with multiple immune checkpoint genes, including HMGB1 and CD276, and then regulate the immune response of tumors, which is projected to be a new target for anti-tumor immunotherapy in the future.

The TME is a precise link between the tumors' occurrence, growth, and metastasis and the internal and external environment of tumor cells and is involved in tumor malignant progression, immune escape, and therapeutic resistance (31). In recent years, therapeutic strategies targeting TME have become a possible method for treating cancer, and its predictive significance has been demonstrated in solid malignancies (32). However, no studies have yet analyzed the connection between *CENPN* and TME. We demonstrated that *CENPN* expression exhibited a negative link to most TIICs aggressiveness, whereas Th2 was significantly positively connected with *CENPN* mRNA expression levels in many cancers. In the TME, it has been demonstrated that patients with less infiltration of anti-tumor lymphocytes (Th1 and CTL) and more infiltration of immunosuppressive lymphocytes (TH2) have a significantly worse prognosis (33). We hypothesized that *CENPN* may influence the poor prognosis of cancer patients by promoting TH2 cell infiltration. Moreover, we found that *CENPN* mRNA expression levels were positively linked to MDSCs invasion levels in many cancers. Because we believe that *CENPN* is correlated with tumor immune cell infiltration, it might be a contributing factor to the worse cancer patients' prognosis.

To get a deeper understanding of the probable mechanism and function of *CENPN* in pan carcinoma, we conducted GO and KEGG enrichment studies of *CENPN*. GO analysis found that its differentially expressed genes were enriched in BP, MF, and CC. KEGG analysis suggested that *CENPN* may mediate neutrophil extranuclear trap formation, cell cycle, and p53 signaling pathways in cancer. Afterward, to investigate the cellular mechanism in more detail, we chose several types of cancer with an adverse connection between prognosis and *CENPN* expression for GSEA analysis. The outcomes demonstrated that *CENPN* expression was primarily linked to positive correlations in DNA methylation, cell cycle, and the TP53 pathway. The S phase is a crucial stage of cell division and proliferation when DNA synthesis takes place (34). In a previous study, by knocking out the *CENPN* expression in human gastric adenocarcinoma cells, it was found that the cell percentage in S and G2-M stages mitigated significantly, which significantly led to the apoptosis of human gastric adenocarcinoma cells (11). In addition, other studies predicted that *CENPN*-related genes were mainly enriched in p53, Rb1, E2F, and other target pathways through the GSEA database. *CENPN* was also demonstrated to regulate LIHC progression by targeting the 21-CDK2/cyclin E, p27-CDK4/cyclin D, and Rb/E2F1 pathways in LIHC cells (9). Combined with the above findings, we conclude that *CENPN* contributes to cancer mainly by affecting the cell cycle TP53 pathway and other biological functions. Our study found that overexpression of *CENPN* elevated the BC cell's proliferation, invasion, and migration and suppressed the BC cells' apoptosis. This offers a new perspective to understand the *CENPN* function and develop new cancer therapies.

Conclusions

In this investigation, the expression, prognosis and diagnosis, epigenetics, methylation, immunoassay, and enrichment analysis of *CENPN* in various tumors were investigated, and it was found that *CENPN* could operate as a novel prognostic marker for malignant tumors and might be a valuable biological target for targeted treatment. Furthermore, we conducted *in vitro* tests to confirm the expression and functional association of *CENPN* in BC. These results improve our knowledge of the function of *CENPN* in cancer and also offer fresh perspectives that might possibly benefit cancer immunotherapy methodologies.

Acknowledgments

None.

Footnote

Reporting Checklist: The authors have completed the

© AME Publishing Company.

TRIPOD and MDAR reporting checklists. Available at https://tcr.amegroups.com/article/view/10.21037/tcr-24-1291/rc

Peer Review File: Available at https://tcr.amegroups.com/article/view/10.21037/tcr-24-1291/prf

Funding: This study received funding from the Regional Collaborative Innovation Special Project (Science and Technology Assistance to Xinjiang Program) (No. 2022E02136), the National Natural Science Foundation of China (No. 32260186), Xinjiang Uygur Autonomous Region Youth Science and Technology Top-notch Talent Program (No. 2022TSYCCX0029), Xinjiang Uygur Autonomous Region Outstanding Youth Science Fund (No. 2024D01E22) and National Health Commission Medical Science and Technology Development Research Center (No. WKZX2023WK0109).

Conflicts of Interest: All authors have completed the ICMJE uniform disclosure form (available at https://tcr.amegroups.com/article/view/10.21037/tcr-24-1291/coif). The authors have no conflicts of interest to declare.

Ethical Statement: The authors are accountable for all aspects of the work in ensuring that questions related to the accuracy or integrity of any part of the work are appropriately investigated and resolved. The study was conducted in accordance with the Declaration of Helsinki (as revised in 2013).

Open Access Statement: This is an Open Access article distributed in accordance with the Creative Commons Attribution-NonCommercial-NoDerivs 4.0 International License (CC BY-NC-ND 4.0), which permits the non-commercial replication and distribution of the article with the strict proviso that no changes or edits are made and the original work is properly cited (including links to both the formal publication through the relevant DOI and the license). See: https://creativecommons.org/licenses/by-nc-nd/4.0/.

References

1. Bray F, Laversanne M, Sung H, et al. Global cancer statistics 2022: GLOBOCAN estimates of incidence and mortality worldwide for 36 cancers in 185 countries. CA Cancer J Clin 2024;74:229-63.
2. Kciuk M, Yahya EB, Mohamed Ibrahim Mohamed M, et al. Recent Advances in Molecular Mechanisms of Cancer Immunotherapy. Cancers (Basel) 2023;15:2721.
3. Perpelescu M, Fukagawa T. The ABCs of CENPs. Chromosoma 2011;120:425-46.
4. Tian T, Li X, Liu Y, et al. Molecular basis for CENP-N recognition of CENP-A nucleosome on the human kinetochore. Cell Res 2018;28:374-8.
5. Allu PK, Dawicki-McKenna JM, Van Eeuwen T, et al. Structure of the Human Core Centromeric Nucleosome Complex. Curr Biol 2019;29:2625-2639.e5.
6. Gui Z, Tian Y, Yu T, et al. Clinical implications and immune features of CENPN in breast cancer. BMC Cancer 2023;23:851.
7. Zheng Y, You H, Duan J, et al. Centromere protein N promotes lung adenocarcinoma progression by activating PI3K/AKT signaling pathway. Genes Genomics 2022;44:1039-49.
8. Wang BR, Han JB, Jiang Y, et al. CENPN suppresses autophagy and increases paclitaxel resistance in nasopharyngeal carcinoma cells by inhibiting the CREB-VAMP8 signaling axis. Autophagy 2024;20:329-48.
9. Wang Q, Yu X, Zheng Z, et al. Centromere protein N may be a novel malignant prognostic biomarker for hepatocellular carcinoma. PeerJ 2021;9:e11342.
10. Wang X, Lai M, Wang Y, et al. Upregulation of Centromere Proteins as Potential Biomarkers for Esophageal Squamous Cell Carcinoma Diagnosis and Prognosis. Biomed Res Int 2022;2022:3758731.
11. Wang X, Zhang K, Fu C, et al. High expression of centromere protein N as novel biomarkers for gastric adenocarcinoma. Cancer Rep (Hoboken) 2023;6:e1798.
12. Goldman MJ, Craft B, Hastie M, et al. Visualizing and interpreting cancer genomics data via the Xena platform. Nat Biotechnol 2020;38:675-8.
13. Lánczky A, Győrffy B. Web-Based Survival Analysis Tool Tailored for Medical Research (KMplot): Development and Implementation. J Med Internet Res 2021;23:e27633.
14. Fang Z, Liu X, Peltz G. GSEApy: a comprehensive package for performing gene set enrichment analysis in Python. Bioinformatics 2023;39:btac757.
15. Chandrashekar DS, Karthikeyan SK, Korla PK, et al. UALCAN: An update to the integrated cancer data analysis platform. Neoplasia 2022;25:18-27.
16. Unberath P, Knell C, Prokosch HU, et al. Developing New Analysis Functions for a Translational Research Platform: Extending the cBioPortal for Cancer Genomics. Stud Health Technol Inform 2019;258:46-50.
17. Liu J, Lichtenberg T, Hoadley KA, et al. An Integrated

TCGA Pan-Cancer Clinical Data Resource to Drive High-Quality Survival Outcome Analytics. Cell 2018;173:400-416.e11.
18. Tate JG, Bamford S, Jubb HC, et al. COSMIC: the Catalogue Of Somatic Mutations In Cancer. Nucleic Acids Res 2019;47:D941-7.
19. Foroutan M, Bhuva DD, Lyu R, et al. Single sample scoring of molecular phenotypes. BMC Bioinformatics 2018;19:404.
20. Zhou K, Gebala M, Woods D, et al. CENP-N promotes the compaction of centromeric chromatin. Nat Struct Mol Biol 2022;29:403-13.
21. Wu H, Zhou Y, Wu H, et al. CENPN Acts as a Novel Biomarker that Correlates With the Malignant Phenotypes of Glioma Cells. Front Genet 2021;12:732376.
22. Zhao Y, Yang J, Zhang N, et al. Integrative analysis of the expression and prognosis for CENPs in ovarian cancer. Genomics 2022;114:110445.
23. Huang TX, Fu L. The immune landscape of esophageal cancer. Cancer Commun (Lond) 2019;39:79.
24. Zhou H, Bian T, Qian L, et al. Prognostic model of lung adenocarcinoma constructed by the CENPA complex genes is closely related to immune infiltration. Pathol Res Pract 2021;228:153680.
25. Chen Z, Li K, Yin X, et al. Lower Expression of Gelsolin in Colon Cancer and Its Diagnostic Value in Colon Cancer Patients. J Cancer 2019;10:1288-96.
26. Sun L, Zhang H, Gao P. Metabolic reprogramming and epigenetic modifications on the path to cancer. Protein Cell 2022;13:877-919.
27. Koch A, Joosten SC, Feng Z, et al. Analysis of DNA methylation in cancer: location revisited. Nat Rev Clin Oncol 2018;15:459-66. Erratum in: Nat Rev Clin Oncol 2018;15:467.
28. Shen P, Han L, Ba X, et al. Hyperprogressive Disease in Cancers Treated With Immune Checkpoint Inhibitors. Front Pharmacol 2021;12:678409.
29. Latham A, Srinivasan P, Kemel Y, et al. Microsatellite Instability Is Associated With the Presence of Lynch Syndrome Pan-Cancer. J Clin Oncol 2019;37:286-95.
30. Samstein RM, Lee CH, Shoushtari AN, et al. Tumor mutational load predicts survival after immunotherapy across multiple cancer types. Nat Genet 2019;51:202-6.
31. Arneth B. Tumor Microenvironment. Medicina (Kaunas) 2019;56:15.
32. Paijens ST, Vledder A, de Bruyn M, et al. Tumor-infiltrating lymphocytes in the immunotherapy era. Cell Mol Immunol 2021;18:842-59.
33. Huang D, Chen X, Zeng X, et al. Targeting regulator of G protein signaling 1 in tumor-specific T cells enhances their trafficking to breast cancer. Nat Immunol 2021;22:865-79.
34. Matthews HK, Bertoli C, de Bruin RAM. Cell cycle control in cancer. Nat Rev Mol Cell Biol 2022;23:74-88.

Cite this article as: Jing Y, Wang Y, Li Y, Huang X, Wang J, Yelihamu D, Guo C. Diagnostics and immunological function of CENPN in human tumors: from pan-cancer analysis to validation in breast cancer. Transl Cancer Res 2025;14(2):881-906. doi: 10.21037/tcr-24-1291

© AME Publishing Company.